



Article

# Optimized Physical Properties of Electrochromic Smart Windows to Reduce Cooling and Heating Loads of Office Buildings

Jae-Hyang Kim <sup>1</sup>, Jongin Hong <sup>2</sup>  and Seung-Hoon Han <sup>3,\*</sup> <sup>1</sup> Graduate School, Chonnam National University, Gwangju 61186, Korea; 101117@jnu.ac.kr<sup>2</sup> Department of Chemistry, Chung-Ang University, Seoul 06974, Korea; hongj@cau.ac.kr<sup>3</sup> School of Architecture, Chonnam National University, Gwangju 61186, Korea

\* Correspondence: hshoon@jnu.ac.kr; Tel.: +82-62-530-1646

**Abstract:** The concept of smart windows that can change the properties of windows and doors in response to external stimuli has recently been introduced. Smart windows provide superior energy savings and control of indoor environments. This concept can advance sustainable architecture, and it will make it possible to connect with the fourth industry, which has developed recently. However, unlike the relevant hardware, is advancing rapidly, research on methods of adjusting smart windows is slow. Therefore, in this study, an analysis of energy use over time was conducted on electrochromic windows, one of the main types of smart windows. Through this analysis, the optimal properties of electrochromic smart windows were identified, and an operation schedule was created. In addition, energy saving rates were derived through a comparison with existing architectural windows.

**Keywords:** electrochromic building component; smart window; heating and cooling loads; energy consumption; sustainable energy utilization



**Citation:** Kim, J.-H.; Hong, J.; Han, S.-H. Optimized Physical Properties of Electrochromic Smart Windows to Reduce Cooling and Heating Loads of Office Buildings. *Sustainability* **2021**, *13*, 1815. <https://doi.org/10.3390/su13041815>

Academic Editors: Farooq Sher, Oliver Curnick and Mohammad Tazli Azizan

Received: 31 December 2020

Accepted: 4 February 2021

Published: 8 February 2021

**Publisher's Note:** MDPI stays neutral with regard to jurisdictional claims in published maps and institutional affiliations.



**Copyright:** © 2021 by the authors. Licensee MDPI, Basel, Switzerland. This article is an open access article distributed under the terms and conditions of the Creative Commons Attribution (CC BY) license (<https://creativecommons.org/licenses/by/4.0/>).

## 1. Introduction

### 1.1. Background and Purpose of the Study

The cooling, heating and lighting loads in buildings are closely related to solar energy. Cooling energy can be saved by blocking solar energy in the summer, and heating energy can be saved by receiving solar energy in the winter. In addition, a pleasant indoor environment is created only when indoor illumination is properly maintained while controlling solar energy. Smart windows with integrated solar control systems are currently under development. Smart windows can adjust the amount of solar energy flowing into the room by changing their material properties in real time. Common categories of smart windows include suspended particle device (SPD), electrochromic, photochromic, and thermochroic windows. Since solar energy is controlled by the glass in such windows, there is no need to go through complex construction processes, and maintenance is also easy. Smart windows can adjust visible light transmittance (VLT) and solar heat gain coefficient (SHGC). The market for these products is growing rapidly. According to the Smart Glass Report by Grand View Research, the total size of the global smart glass market was estimated at \$3,710,000,000 in 2018, and is expected to record an annual average growth rate of about 15.2% from 2019 to 2025 [1].

Representative materials used for smart windows are SPD and electrochromic glass. Electrochromic glass operates at low voltages and is highly durable, so it is entering the commercialization stage as architectural windows. However, it is difficult to establish an energy savings plan using smart windows because the amount of architectural research that has been done is insufficient compared to that of material development research. In addition, research on the energy performance data of windows and doors is needed to operate smart windows.

Therefore, this study aims to analyze the energy performance of an indoor space according to changes in the physical properties of electrochromic smart windows, and to analyze the rate at which energy can be saved by the use of smart windows rather than existing windows. Since electrochromic glass has a wide VLT range and good g-value control, its use leads to significant energy savings if appropriate values are set according to the season and time. However, there is insufficient research into such optimal values. In this study, the most efficient electrochromic window operation schedule was determined by calculating the heating and cooling energy load on the spring equinox, summer solstice, autumn equinox and winter solstice, which are representative days of the four seasons. In addition, the energy savings rate was analyzed in comparison to existing windows.

### 1.2. Background

Research on the applications of electrochromic smart windows in the architecture realm mainly includes indoor environment analysis and energy analysis. Nuria and colleagues conducted a comparative analysis on the optical and thermal characteristics of semi-transparent PV modules and electrochromic windows that can be used in buildings [2]. Abdelsalam calculated solar heat gains in hot and dry climates for three control groups (overhangs, overhangs and side fins, and electrochromic glazing), and demonstrated the benefits of electrochromic compared to shading devices [3]. Dussault et al. analyzed the sensitivity of energy performance and thermal and visual comfort for office buildings with electrochromic windows [4]. Kim et al. conducted a partial color environment analysis of blue-type electrochromic windows [5]. Nicholas et al. analyzed the energy efficiency of commercial and residential buildings across the United States for three electrochromic states, “dark”, “cool” and “bright” [6]. Oh et al. calculated and compared the monthly energy load using models of electrochromic glass, general glass, blinds, and roll shades. Those authors showed that the use of electrochromic glass resulted in inferior heating load compared to other shade devices, but electrochromic glass had a remarkably strong positive effect on the cooling load [7]. In another study by the same authors, the temperature and solar energy of electrochromic glass were analyzed in three randomly selected cities, Moscow, Incheon, and Riyadh. In addition, the natural lighting performance of electrochromic glass was derived, which was then analyzed using the energy and daylight performance index (EDPI) [8]. In Michaela et al., the annual energy load of a building with a high window-to-wall ratio (WWR) was analyzed for six different thermochromic and electrochromic combinations [9]. In a study by Cannavale, the cooling and lighting loads of electrochromic, photochromic, thermochromic, clear, tinted, and reflective glass were compared and analyzed. The findings demonstrated the suitability of electrochromic glass as a smart architectural window [10]. In that research, attention was paid to the lighting and energy performance of electrochromic glass. However, there was insufficient analysis of the factors that changed the properties of electrochromic glass. Also, since these studies were conducted based on yearly analyses, a basic understanding of the operating principles of electrochromic glass over time is needed.

Another research direction in the smart window realm is the analysis of SPD, which shows similar performance to electrochromic glass. In Ghosh et al., a mock-up was created, and its overall physical properties were analyzed to assess changes in the wavelength and temperature of incident sunlight for two SPD states (VLT 5% and VLT 55%) [11]. Nundy and colleagues compared the physical properties, such as wavelength and temperature, of double-glazed windows, SPD, and Vacuum-SPD [12]. In Min et al., simulation analysis was conducted on the cooling load in summer for the U-value of SPD and the maximum and minimum values of SHGC [13]. Ko et al. evaluated the energy performance of smart windows according to the WWR and the g-value range of SPD [14]. The evaluation was done with the TRNSYS18 simulation program, and a range of g-values according to the WWR was proposed. In another study by Ko et al., a SPD-based mock-up was constructed, and the measured data from the mock-up were compared to the simulation results [15].

The evaluation of the energy performance of a building is mostly based on an energy simulation or test bed operation. In a study by Baek and colleagues, the cooling and heating loads were analyzed to determine the optimal design of a folding awning device, and the integrated analysis program IES\_VE (Integrated Environmental Solutions\_Virtual Environment) was used [16]. The cooling and heating loads were calculated through modeling according to the shape of the awning and the length of the protrusion, and the superiority of the folding awning was verified by comparison with an existing awning. In a study by Park et al., the heat acquisition and heat loss of windows were analyzed using the EnergyPlus program [17]. Simulated data on heat acquisition and heat loss of the lower extremities on the winter solstice were derived according to the composition of the windows and the type of shade, and the maximum cooling and heating loads were calculated and compared. Kim et al. proposed a hybrid heating, ventilation, and air conditioning (HVAC) system for a skyscraper office building, and tried to demonstrate its superiority through simulation with TRNSYS [18]. Those authors developed an air cap wall module for energy reduction, constructed a test bed, and compared and analyzed lighting energy and cooling/heating energy according to the thickness of the air cap wall [19].

## 2. Research Analysis Framework

### 2.1. Method and Flow

This study aims to analyze the operation schedule considering the cooling and heating energy performance of electrochromic smart windows and the energy savings rate compared to existing architectural windows. Therefore, to compare the cooling and heating energy performance, groups of electrochromic smart windows and existing architectural windows with various g-values and U-values were established. Analysis was done through simulations. Based on previous research, an EnergyPlus engine was used to derive the energy consumption over time. In addition, Rhino Grasshopper's Ladybug Plug-in was applied to efficiently organize data on the cooling and heating loads of each control group. The Ladybug plug-in, which can apply the EnergyPlus engine to the Rhino Grasshopper model, is capable of extracting and organizing the values of the required data. After setting up the simulation program, the simulation area and analysis point were set, and a virtual target building was created. For the southern, eastern and western sides, the cooling energy and heating energy consumption of the control groups were derived over time. Based on this data, a g-value schedule was created for optimal operation of electrochromic smart windows, and the total amount of energy consumed was calculated. The energy savings rate of the smart windows compared to the existing windows was compared through the calculated values. The flow of research is shown in Figure 1.

### 2.2. Test Configuration

#### 2.2.1. Specimen Configuration

Cooling and heating loads are determined by a comprehensive array of factors, such as the construction of the building and facilities. For windows, U-value, g-value, and airtightness are recognized as factors that affect the cooling and heating loads. Since airtightness depends on the composition of the window frame, it was assumed to be the same across groups in this study. Therefore, variables representing the U-value and g-value were used to compare electrochromic smart windows and existing windows. The U-value and g-value of the electrochromic smart windows were determined based on the products currently on the market. Electrochromic smart windows are composed of multiple layers of functional glass, and the U-value and g-value were 1.1 W/m<sup>2</sup>k and 0.12–0.44, respectively [15]. If the g-value of an electrochromic window is set to either the maximum or minimum, durability may be impaired. Therefore, the g-values of the control group were set at 0.05-unit intervals in the range of 0.15 to 0.40, which are realistic values. The three control groups of existing windows were Clear glass + Clear glass, LowE glass + Clear glass, and LowE glass + LowE glass, and a glass thickness of 24 mm was used for

all control groups. The properties of each glass were combined and calculated from an EnergyPlus-based library. Details of the control groups are shown in Table 1.

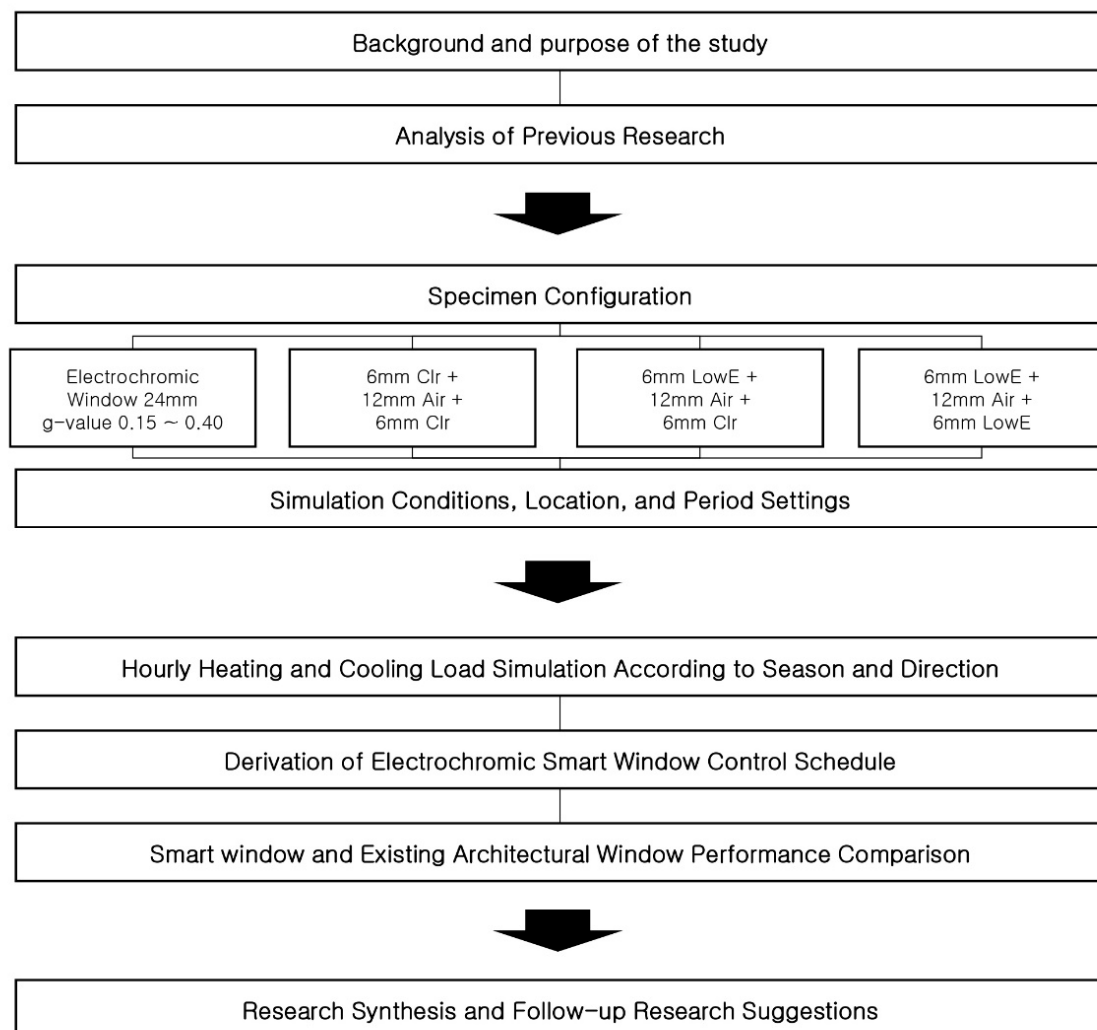


Figure 1. Research flow.

Table 1. Details of control windows.

Division	g-Value	U-Value (W/m <sup>2</sup> ·k)
24 mm Electrochromic Window (EC)	0.15~0.40 (Interval 0.05)	1.1
6 mm Clr + 12 mm Air + 6 mm Clr (CC)	0.703	2.685
6 mm Clr + 12 mm Air + 6 mm LowE (CL)	0.568	1.771
6 mm LowE + 12 mm Air + 6 mm LowE (LL)	0.488	1.165

### 2.2.2. Analysis Site and Time Configuration

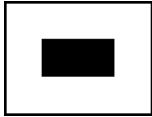


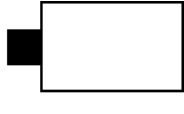


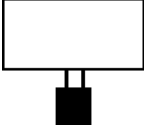
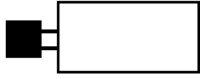

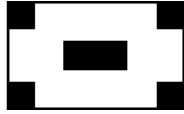
The location of the simulation was set to Gwangju, Korea, and the 2015 Gwangju Weather Data EnergyPlus Weather (EPW) file provided by the Korea Passive Architecture Association was used to obtain data [20]. The purpose of this study is to analyze the cooling and heating energy load by season, so simulations were performed on the spring equinox, summer solstice, autumnal equinox, and winter solstice, which represent the four seasons. However, individual EPW files may reflect special weather events such as snow or rain. Therefore, if the data from the equinox or solstice did not represent the season as a whole,

the data for the closest possible date that was representative was used. Based on the 2015 EPW, the data from 16 March, 19 June, 26 September, and 21 December were used.

### 2.2.3. Office Unit Configuration

The configuration of an office building can differ depending on the type of core, and is the most basic element to consider when composing a useful space. The core space is planned according to the location and number of cores, and the core type affects the size of the base floor and the ways in which the office space can be used. According to the core plan, office buildings are divided into central, eccentric, both ends, independent, and distributed core type; the features of each are shown in Table 2 [21].

**Table 2.** Core types and features.

Division	Configuration	Features
Central core type	 	<ul style="list-style-type: none"> <li>- Structurally most advantageous</li> <li>- View, natural light glass</li> <li>- Increased cooling &amp; heating load</li> <li>- High effective rate</li> </ul>
Eccentric core type	 	<ul style="list-style-type: none"> <li>- Suitable when the standard floor area is small</li> <li>- No dynamic exterior on 4 sides</li> </ul>
Both ends core type	 	<ul style="list-style-type: none"> <li>- Suitable for single-use large-scale dedicated offices</li> <li>- Disaster prevention/evacuation phase glass for 2-way evacuation</li> <li>- Skin load reduction</li> </ul>
Independent core type	 	<ul style="list-style-type: none"> <li>- Almost the same features as eccentric core type</li> <li>- Less core interference in the office space layout</li> <li>- Facility planning disadvantage</li> </ul>
Distributed core type	 	<ul style="list-style-type: none"> <li>- Advantageous responsiveness to changes in office space</li> <li>- Disaster prevention glass</li> <li>- Increased construction cost</li> </ul>

In this study, the area of the core was calculated as 81 m<sup>2</sup>; it was a 9 × 9 m<sup>2</sup> square. The span of the office pillar can be calculated by the parking space, and it was calculated as 8.1 m considering the three sides of the parking space and the size of the pillar (2.5 × 3 + 0.6 m). The width of the office space was 6 m, which was determined by subtracting the 2.1 m of corridor space from the 8.1 m column spacing span. The height was set to 3.4 m, and the ceiling height was set to 2.6 m. The window area ratio was 60%. A schematic illustration of the created office is shown in Figure 2.

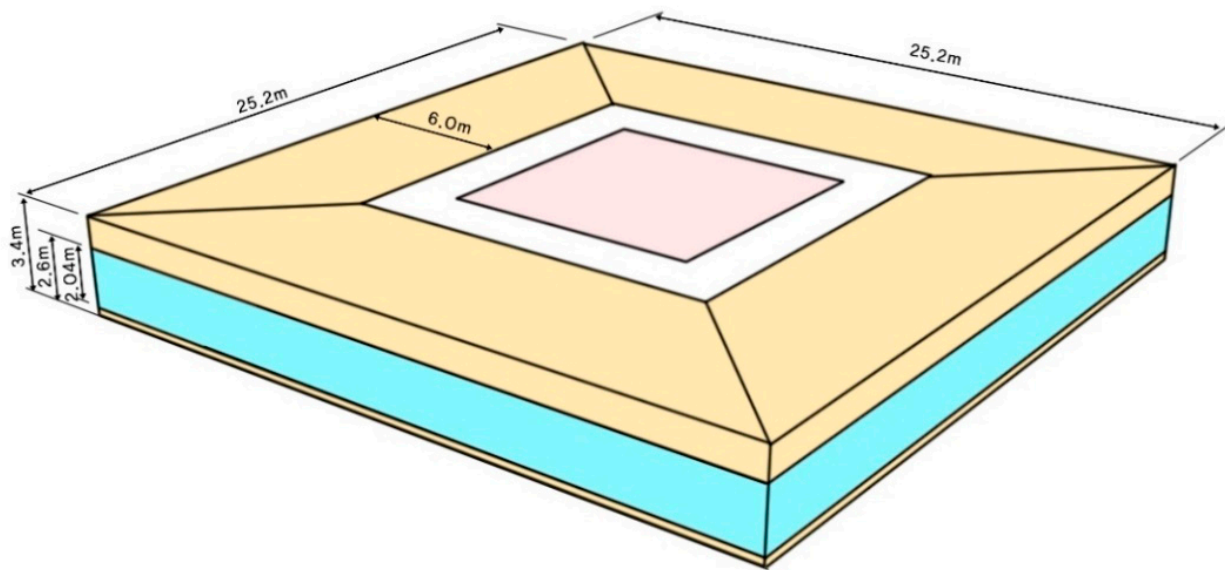


Figure 2. Simulation unit.

The composition of the wall, floor, and roof is based on the energy conservation design standard. The physical properties of the material and the heat transmission rate standards for non-residential southern regions are shown in Table 3 [22].

Table 3. Physical properties of the office unit structure.

Division		Thickness (mm)	Thermal Conductivity (W/m·K)	Density (kg/m <sup>3</sup> )	Specific Heat (kJ/kg·K)	Heat Resistance (m <sup>2</sup> ·K/W)	Heat Transmission Rate (W/m <sup>2</sup> ·K)
Outer Wall	Granite	20	3	2810	0.84	3.814	0.297
	Insulator	100	0.034	30	1.417		
	Concrete	200	1.6	2200	0.88		
Roof	Concrete	200	1.6	2200	0.88	5.839	0.171
	Insulator	180	0.034	30	1.417		
	Ceiling frame	30	0.14	360	1.6		
	Gypsum board	9.5	0.18	10	1		
Floor	Granite	30	3	2810	0.84	2.858	0.350
	Mortar	40	1.4	2000	0.89		
	Lightweight aerated concrete	40	0.19	400	0.88		
	Insulator	70	0.034	30	1.417		
	MAT concrete	500	1.6	2200	0.88		
External surface heat resistance						0.043	-
Inner surface heat resistance						0.11	-

A facility that can be used in general office buildings was planned, and an air-cooled refrigerator and hot water boiler were set up as heat sources. In addition, a variable air volume (VAV) reheating system with excellent energy savings was adopted, which was composed of a single duct. The immersion rate was set to 0.22 times/h. The heat densities generated by human body heat, lighting, and equipment were set to 65, 11, and 21 W/m<sup>2</sup>, respectively. The operation schedule was set based on ASHRAE 90.1. A summary of the simulation settings is shown in Table 4.

**Table 4.** Simulation settings.

Division		Contents
Facility system	Heat source equipment	Air flow freezer, hot water boiler
	Air conditioning equipment	VAV reheating system, single duct
Infiltration		0.22 times/h
Human body fever		65 W/m <sup>2</sup>
Lighting fever		11 W/m <sup>2</sup>
Device fever		21 W/m <sup>2</sup>

### 3. Simulation Results and Analysis

#### 3.1. South Side Analysis

##### 3.1.1. Spring Equinox Analysis

On the south side of the building on the spring equinox, both cooling energy and heating energy were required. The total daily cooling and heating loads are shown in Table 5.

**Table 5.** Energy load of the south side on the spring equinox (cooling/heating) (W/m<sup>2</sup>).

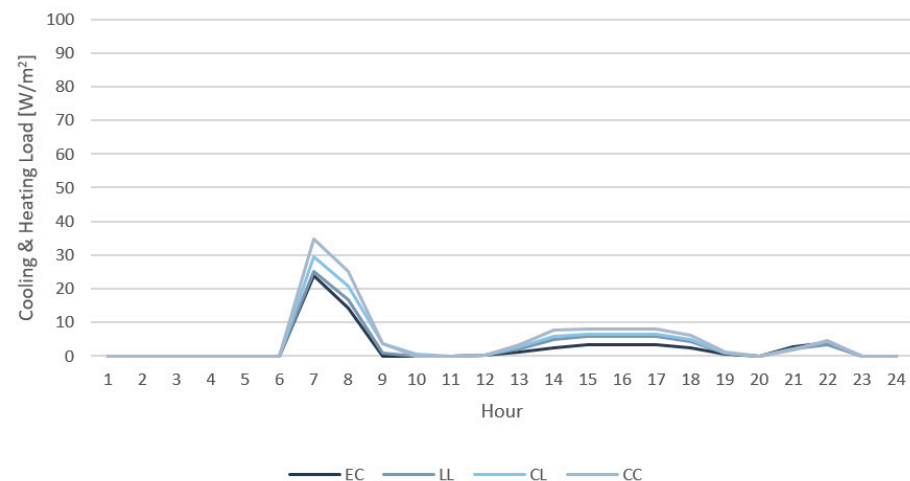
Time	Electrochromic Smart Window (U-Value 1.1)					Architectural Window (U-Value 2.685, 1.771, 1.165)			
	EC (0.15)	EC (0.20)	EC (0.25)	EC (0.30)	EC (0.35)	EC (0.40)	CC (0.70)	CL (0.57)	LL (0.49)
1	0/0	0/0	0/0	0/0	0/0	0/0	0/0	0/0	0/0
2	0/0	0/0	0/0	0/0	0/0	0/0	0/0	0/0	0/0
3	0/0	0/0	0/0	0/0	0/0	0/0	0/0	0/0	0/0
4	0/0	0/0	0/0	0/0	0/0	0/0	0/0	0/0	0/0
5	0/0	0/0	0/0	0/0	0/0	0/0	0/0	0/0	0/0
6	0/0.299	0/0	0/0	0/0	0/0	0/0	0/0	0/0	0/0
7	0/29.731	0/25.861	0/23.997	0/23.733	0/23.773	0/24.823	0/34.701	0/29.386	0/25.207
8	0/17.269	0/15.269	0/14.205	0/14.346	0/14.665	0/15.915	0/25.185	0/20.606	0/16.82
9	0/0.35	0/0	0/0	0/0	0/0	0/0	0/3.551	0/3.683	0/0.978
10	0/0	0/0	0/0	0/0	0/0	0/0	0/0	0/0.534	0/0
11	0/0	0/0	0/0	0/0	0/0	0/0	0/0	0/0	0/0
12	0.086/0	0.096/0	0.107/0	0.119/0	0.132/0	0.136/0	0.216/0	0.177/0	0.155/0
13	1.232/0	1.38/0	1.538/0	1.719/0	1.99/0	1.961/0	3.483/0	2.595/0	2.242/0
14	2.501/0	2.807/0	3.334/0	3.933/0	4.543/0	4.228/0	7.529/0	5.899/0	4.783/0
15	3.216/0	3.607/0	4.006/0	4.456/0	4.926/0	5.055/0	7.855/0	6.532/0	5.68/0
16	3.332/0	3.737/0	4.006/0	4.456/0	4.926/0	5.055/0	7.855/0	6.532/0	5.68/0
17	3.337/0	3.741/0	4.006/0	4.456/0	4.926/0	5.055/0	7.855/0	6.532/0	5.68/0
18	2.373/0	2.659/0	2.973/0	3.324/0	3.692/0	3.793/0	5.987/0	4.95/0	4.337/0
19	0.442/2.601	0.496/1.312	0.551/0	0.616/0	0.684/0	0.703/0	1.109/0	0.917/0	0.803/0
20	0/3.934	0/2.203	0/0.334	0/0	0/0	0/0	0/0	0/0	0/0
21	0/9.605	0/8.077	0/5.698	0/4.153	0/2.711	0/3.729	0/1.737	0/2.168	0/1.961
22	0/10.151	0/8.771	0/6.666	0/5.297	0/4.074	0/5.012	0/4.494	0/4.302	0/3.373
23	0/0	0/0	0/0	0/0	0/0	0/0	0/0	0/0	0/0
24	0/0	0/0	0/0	0/0	0/0	0/0	0/0	0/0	0/0
Total	90.459	80.016	71.421	70.608	71.042	75.465	111.557	94.813	77.699

The g-value of smart windows that minimizes the load was derived for each hour, taking into account both cooling and heating energy. From 0 to 5 o'clock, the load was calculated as 0 regardless of the g-value, and from 5 to 6 o'clock, the load was also 0 except for at a g-value of 0.15. The best g-value at 6 to 7 o'clock was 0.30, and the best g-value at 7 to 8 o'clock was 0.25. At 8 to 9 o'clock, the load was 0 except for at a g-value of 0.15, and from 9 to 11 o'clock the load was 0 regardless of the g-value. From 11 to 18 o'clock, the g-value 0.15 corresponded to the lowest load, and from 18 to 19 o'clock, the g-value of 0.25 corresponded to the lowest load. From 19 to 20 o'clock, for all g-values over 0.30, the load was calculated as 0, and between 20 and 22 o'clock, the g-value of 0.35 corresponded to the lowest load. Finally, after 22 o'clock, the load was 0 regardless of the g-value. The final schedule is shown in Table 6. For times with the same load, a lower g-value was adopted for privacy purposes at night, and a higher g-value was adopted for mining during the day.

**Table 6.** Smart window g-value schedule for the south side on the spring equinox.

Time	1	2	3	4	5	6	7	8	9	10	11	12
g-value	0.15	0.15	0.15	0.15	0.15	0.40	0.30	0.25	0.40	0.40	0.40	0.15
Time	13	14	15	16	17	18	19	20	21	22	23	24
g-value	0.15	0.15	0.15	0.15	0.15	0.15	0.25	0.30	0.35	0.35	0.15	0.15

When the schedule was applied, the minimum value of the cooling and heating load was calculated as  $61.351 \text{ W/m}^2$ , while that of the existing building windows CC, CL, and LL were calculated as  $111.557$ ,  $94.813$ , and  $77.699 \text{ W/m}^2$ , respectively. Thus, the use of smart windows rather than control windows could reduce the cooling and heating loads by 21.0% to 45.0% on the spring equinox. A graph comparing the energy load of the electrochromic window applied using the derived schedule to that of control windows is shown in Figure 3.



**Figure 3.** Energy load comparison on the south side on the spring equinox.

### 3.1.2. Summer Solstice Analysis

On the summer solstice, only cooling energy was required. In most cases, we found that the lower the g-value, the lower the cooling load. The total daily cooling load is shown in Table 7.



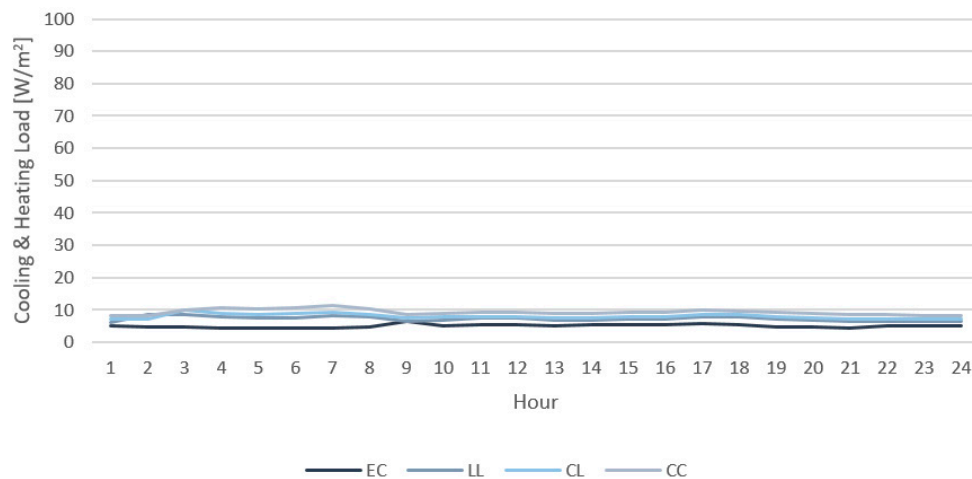
**Table 7.** Energy load of the south side on the summer solstice (cooling) ( $W/m^2$ ).

Time	Electrochromic Smart Window (U-Value 1.1)						Architectural Window (U-Value 2.685, 1.771, 1.165)		
	EC (0.15)	EC (0.20)	EC (0.25)	EC (0.30)	EC (0.35)	EC (0.40)	CC (0.70)	CL (0.57)	LL (0.49)
1	4.836	5.428	6.222	6.599	6.518	6.685	8.19	6.981	6.218
2	4.778	5.36	6.131	6.859	7.622	7.833	8.136	6.936	8.656
3	4.591	5.138	5.846	6.54	7.269	7.47	9.779	9.758	8.564
4	4.322	4.787	5.267	5.893	6.55	6.731	10.654	8.797	7.717
5	4.271	4.73	5.121	5.727	6.364	6.54	10.342	8.542	7.49
6	4.298	4.76	5.198	5.815	6.462	6.64	10.506	8.677	7.61
7	4.456	4.97	5.613	6.28	6.981	7.174	11.313	9.364	8.225
8	4.687	5.254	6.007	6.719	7.466	7.3	10.158	8.441	7.883
9	6.313	6.559	6.658	6.759	6.839	6.855	8.618	7.338	6.507
10	5.152	5.373	5.615	5.84	6.237	6.33	8.898	7.642	6.892
11	5.503	5.717	6.097	6.267	6.651	6.759	9.182	7.943	7.296
12	5.53	5.785	6.214	6.454	6.736	6.762	9.26	7.948	7.309
13	4.928	5.227	5.424	5.743	6.201	6.204	8.893	7.536	6.77
14	5.194	5.484	5.632	5.942	6.333	6.144	8.857	7.46	6.681
15	5.349	5.623	5.779	6.069	6.458	6.557	9.217	7.875	7.149
16	5.498	5.787	6.043	6.339	6.698	6.752	9.246	7.967	7.23
17	5.857	6.144	6.604	6.873	7.195	7.214	9.763	8.464	7.745
18	5.407	5.695	6.091	6.434	6.934	7.069	9.723	8.456	7.777
19	4.742	5.169	5.578	6.03	6.458	6.567	9.219	7.916	7.177
20	4.51	4.912	5.108	5.517	5.96	6.085	8.793	7.518	6.729
21	4.302	4.692	4.754	5.199	5.667	5.797	8.469	7.217	6.434
22	5.071	5.258	5.022	5.099	5.564	5.694	8.343	7.104	6.326
23	5.205	5.861	6.273	5.082	5.547	5.676	8.312	7.08	6.307
24	5.146	5.792	6.67	5.087	5.549	5.678	8.291	7.072	6.304
Total	119.946	129.505	138.967	145.166	156.259	158.516	222.162	190.032	172.996

From 21 to 22 o'clock, when the g-value is 0.25, the cooling load is lowest, and from 22 to 24 o'clock, when the g-value is 0.30, the cooling load is the lowest. The total daily cooling load of smart windows with a g-value of 0.15 was the lowest, at  $119.946 W/m^2$ . In addition, when the schedule in Table 8 was applied, the daily cooling load was calculated as  $119.715 W/m^2$ . The cooling load of the control windows CC, CL, and LL was calculated as  $222.162$ ,  $190.032$ , and  $172.996 W/m^2$ , respectively. Thus, application of smart windows on the south side of the building on the summer solstice can reduce the cooling load by 30.8% to 46.1%. A graph comparing the energy load of the electrochromic window applied using the derived schedule vs. that of the control windows is shown in Figure 4.

**Table 8.** Smart window g-value schedule for the south side on the summer solstice.

Time	1	2	3	4	5	6	7	8	9	10	11	12
g-value	0.15	0.15	0.15	0.15	0.15	0.15	0.15	0.15	0.15	0.15	0.15	0.15
Time	13	14	15	16	17	18	19	20	21	22	23	24
g-value	0.15	0.15	0.15	0.15	0.15	0.15	0.15	0.15	0.15	0.25	0.30	0.30

**Figure 4.** Energy load comparison for the south side on the summer solstice.

### 3.1.3. Autumnal Equinox Analysis

On the autumnal equinox, both cooling energy and heating energy were required, and the cooling load was greater than that on the spring equinox. The total daily cooling and heating load is shown in Table 9.

**Table 9.** Energy load on the south side on the autumnal equinox (cooling/heating) ( $W/m^2$ ).

Time	Electrochromic Smart Window (U-Value 1.1)						Architectural Window (U-Value 2.685, 1.771, 1.165)		
	EC (0.15)	EC (0.20)	EC (0.25)	EC (0.30)	EC (0.35)	EC (0.40)	CC (0.70)	CL (0.57)	LL (0.49)
1	1.893/0	2.124/0	2.391/0	2.674/0	2.97/0	3.052/0	4.821/0	3.984/0	3.492/0
2	1.985/0	2.225/0	2.494/0	2.789/0	3.098/0	3.183/0	5.026/0	4.154/0	3.64/0
3	1.443/0	1.617/0	1.803/0	2.016/0	2.239/0	2.301/0	3.631/0	3.002/0	2.63/0
4	1.071/0	1.204/0	1.372/0	1.535/0	1.706/0	1.753/0	2.773/0	2.29/0	2.008/0
5	1.068/0	1.202/0	1.373/0	1.536/0	1.707/0	1.754/0	2.774/0	2.291/0	2.009/0
6	0.643/0	0.722/0	0.812/0	0.908/0	1.009/0	1.036/0	1.636/0	1.353/0	1.185/0
7	0.495/4.344	0.555/2.959	0.62/2.139	0.694/1.924	0.77/1.794	0.792/2.36	1.25/5.965	1.033/3.946	0.905/2.439
8	1.385/0.375	1.554/0	1.752/0	1.959/0	2.177/0	2.237/0	3.534/1.062	2.92/0.473	2.559/0
9	3.158/0	3.529/0	3.709/0	4.137/0	4.583/0	4.706/0	7.371/0	6.111/0	5.333/0
10	3.839/0	4.208/0	4.006/0	4.456/0	4.926/0	5.055/0	7.855/0	6.532/0	5.68/0
11	3.839/0	4.219/0	4.148/0	4.635/0	5.151/0	5.081/0	8.086/0	6.582/0	5.688/0
12	4.005/0	4.474/0	4.616/0	5.18/0	5.79/0	5.557/0	9.228/0	7.308/0	6.152/0

Table 9. Cont.

Time	Electrochromic Smart Window (U-Value 1.1)						Architectural Window (U-Value 2.685, 1.771, 1.165)		
	EC (0.15)	EC (0.20)	EC (0.25)	EC (0.30)	EC (0.35)	EC (0.40)	CC (0.70)	CL (0.57)	LL (0.49)
13	4.08/0	4.601/0	4.813/0	5.461/0	6.156/0	5.929/0	10.152/0	7.956/0	6.621/0
14	4.417/0	5.013/0	5.347/0	6.1/0	6.896/0	6.536/0	11.459/0	8.845/0	7.313/0
15	4.352/0	4.974/0	5.351/0	6.154/0	6.996/0	6.436/0	11.692/0	8.792/0	7.268/0
16	4.171/0	4.76/0	5.098/0	5.881/0	6.703/0	6.06/0	11.165/0	8.276/0	6.937/0
17	3.982/0	4.464/0	4.651/0	5.295/0	5.992/0	5.695/0	9.908/0	7.639/0	6.544/0
18	3.839/0	4.208/0	4.031/0	4.492/0	4.996/0	5.098/0	8.208/0	6.673/0	5.778/0
19	3.839/0	4.211/0	4.039/0	4.495/0	4.97/0	5.1/0	7.932/0	6.594/0	5.736/0
20	3.768/0	4.161/0	4.006/0	4.456/0	4.926/0	5.055/0	7.855/0	6.532/0	5.68/0
21	3.024/0	3.391/0	3.749/0	4.184/0	4.639/0	4.765/0	7.482/0	6.197/0	5.415/0
22	2.391/0	2.682/0	3.008/0	3.363/0	3.736/0	3.839/0	6.062/0	5.01/0	4.39/0
23	2.071/0	2.322/0	2.599/0	2.906/0	3.228/0	3.317/0	5.236/0	4.328/0	3.792/0
24	1.792/0	2.009/0	2.245/0	2.509/0	2.787/0	2.864/0	4.521/0	3.737/0	3.274/0
Total	71.269	77.388	80.172	89.739	99.945	99.561	166.684	132.558	112.468

The g-value of smart windows that can minimize the load was derived for each hour, taking into account both cooling and heating energy. Excluding 6 to 8 o'clock, smart windows with a g-value of 0.15 showed the lowest cooling and heating load, and between 6 and 7 o'clock, a g-value of 0.35 was the most advantageous. In addition, a g-value of 0.20 is the most advantageous in terms of energy use at 7–8 o'clock. The final schedule is shown in Table 10.

Table 10. Smart window g-value schedule for the south side on the autumnal equinox.

Time	1	2	3	4	5	6	7	8	9	10	11	12
g-value	0.15	0.15	0.15	0.15	0.15	0.40	0.30	0.25	0.40	0.40	0.40	0.15
Time	13	14	15	16	17	18	19	20	21	22	23	24
g-value	0.15	0.15	0.15	0.15	0.15	0.15	0.25	0.30	0.35	0.35	0.15	0.15

When the schedule was applied, the minimum value of the cooling and heating load was 68.788 W/m<sup>2</sup>, while those of the existing building windows CC, CL, and LL were 166.684, 132.558, and 112.468 W/m<sup>2</sup>. Thus, we found that the cooling and heating loads could be reduced by 38.8–58.7% when smart windows were used instead of control windows on the autumnal equinox on the south side. A graph comparing the energy load of the electrochromic window applied with the schedule to those of the control windows is shown in Figure 5.

### 3.1.4. Winter Solstice Analysis

On the winter solstice, only heating energy was required. The total daily heating load is shown in Table 11.

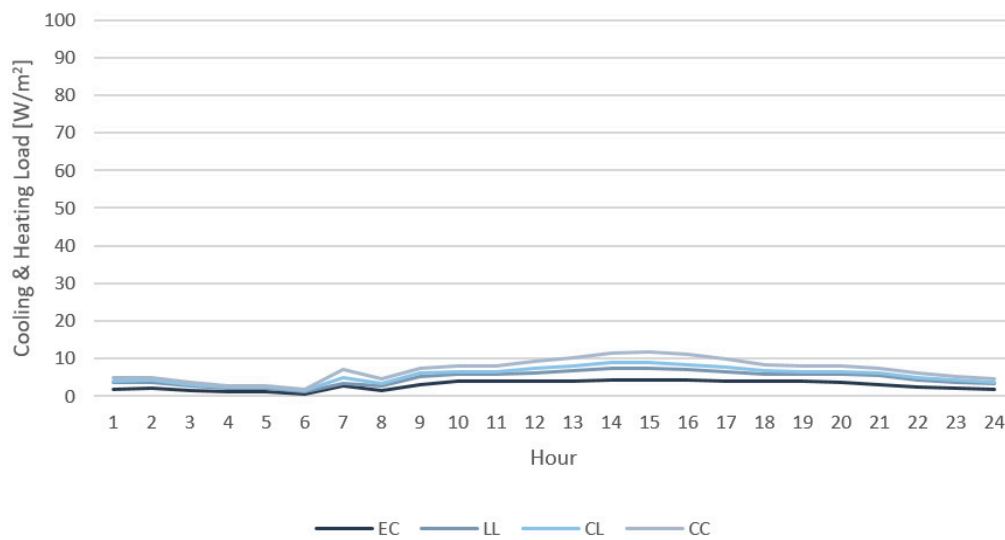


Figure 5. Energy load comparison on the south side on the autumnal equinox.

Table 11. Energy load on the south side on the winter solstice (heating) ( $W/m^2$ ).

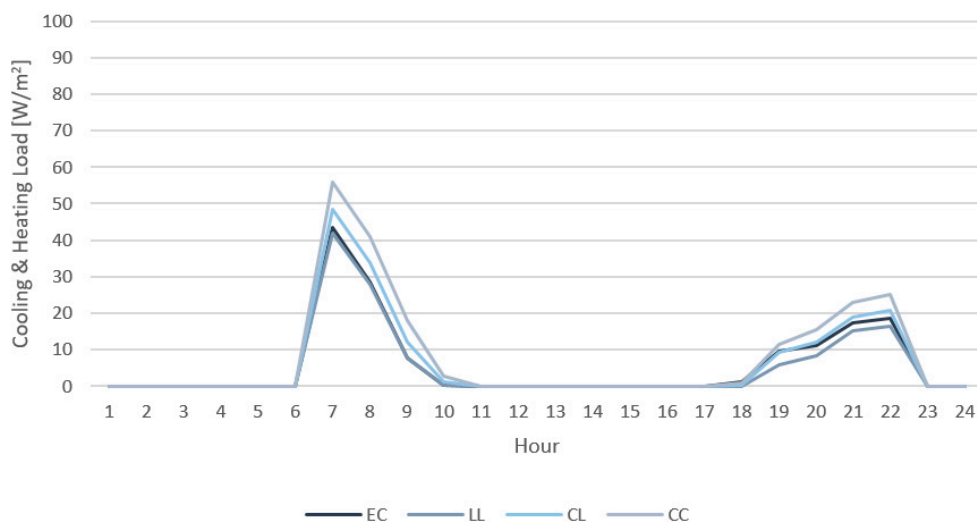
Time	Electrochromic Smart Window (U-Value 1.1)						Architectural Window (U-Value 2.685, 1.771, 1.165)		
	EC (0.15)	EC (0.20)	EC (0.25)	EC (0.30)	EC (0.35)	EC (0.40)	CC (0.70)	CL (0.57)	LL (0.49)
1	2.308	0.917	0	0	0	0	0	0	0
2	2.31	0.918	0	0	0	0	0	0	0
3	3.084	0.92	0	0	0	0	0	0	0
4	3.804	0.921	0	0	0	0	0	0	0
5	4.547	1.318	0	0	0	0	0	0	0
6	5.158	2.055	0	0	0	0	0	0	0
7	57.589	56.043	53.992	49.962	46.428	43.582	56.003	48.533	41.883
8	37.292	35.971	33.952	32.101	30.118	28.389	41.002	33.767	27.994
9	16.655	14.982	12.71	10.708	8.664	7.759	17.899	12.082	7.547
10	8.745	6.202	3.266	1.16	0.404	0.343	2.562	1.176	0.298
11	6.777	3.875	1.197	0	0	0	0	0	0
12	0.692	0	0	0	0	0	0	0	0
13	0	0	0	0	0	0	0	0	0
14	0	0	0	0	0	0	0	0	0
15	0	0	0	0	0	0	0	0	0
16	1.23	0	0	0	0	0	0	0	0
17	6.174	2.62	0.436	0	0	0	0	0	0
18	15.093	12.268	9.312	6.552	3.71	1.307	0.948	0.327	0
19	22.28	19.827	17.157	15.011	12.114	9.415	11.486	9.135	5.889
20	22.752	20.544	18.064	16.184	13.638	11.135	15.359	12.006	8.317
21	28.137	26.089	23.756	22.003	19.782	17.426	23.02	18.993	15.019
22	28.489	26.609	24.406	22.686	20.758	18.506	25.121	20.584	16.361
23	2.358	1.003	0	0	0	0	0	0	0
24	2.297	0.912	0	0	0	0	0	0	0
Total	277.771	233.994	198.248	176.367	155.616	137.862	193.4	156.603	123.308

Among the control groups, the LL architectural windows were the most efficient, and the CC and CL windows with relatively high U-values were found to have increased

heating load despite their high g-values. For the smart windows, the higher the g-value, the lower the heating load; even if the g-value was low in a certain section, the heating load was calculated as 0. When the schedule in Table 12 was applied, the daily heating load was  $137.862 \text{ W/m}^2$ , which was higher than that of LL architectural windows but more efficient than CC and CL windows. Smart windows to which the schedule was applied have a 11.8% higher heating load than LL architectural windows. Therefore, the heating load can be reduced by 12.0–28.7% when smart windows are used rather than CC and CL windows. A graph comparing the energy load of the electrochromic window applied with the schedule to those of the control windows is shown in Figure 6.

**Table 12.** Smart window g-value schedule for the south side on the winter solstice.

Time	1	2	3	4	5	6	7	8	9	10	11	12
g-value	0.25	0.2	50.25	0.25	0.25	0.25	0.40	0.40	0.40	0.40	0.40	0.40
Time	13	14	15	16	17	18	19	20	21	22	23	24
g-value	0.40	0.40	0.40	0.40	0.40	0.40	0.40	0.40	0.40	0.40	0.25	0.25



**Figure 6.** Energy load comparison on the south side on the winter solstice.

### 3.2. East Side Analysis

#### 3.2.1. Spring Equinox Analysis

On the east side of the building on the spring equinox, both cooling energy and heating energy were required. The total daily cooling and heating load is shown in Table 13.

The g-value of smart windows that can minimize the load was derived for each hour, taking into account both cooling and heating energy. From 0 to 6 o'clock, the load was calculated as 0 regardless of the g-value, and at 6 to 7 o'clock, the best g-value was 0.40. The g-value of 0.30 was the best at 7 to 8 o'clock. At 8 to 12 o'clock, the load was 0 regardless of the g-value, and at 11 to 12 o'clock, a g-value 0.15 was found to be the most efficient. From 12 to 13 o'clock, a g-value of 0.20 was associated with the lowest load, and at 13 to 17 o'clock, the g-value of 0.15 corresponded to the lowest load. From 17 to 18 o'clock, a g-value of 0.25 produced the lowest load; at 18 to 22 o'clock, a g-value of 0.40 produced the lowest load; and at 21 to 22 o'clock, a g-value of 0.20 corresponded to the lowest load. After 22:00, the load was calculated as 0 regardless of the g-value. The final schedule is shown in Table 14. For times with the same load, a lower g-value was adopted for privacy purposes at night, and a higher g-value was adopted for mining during the day.

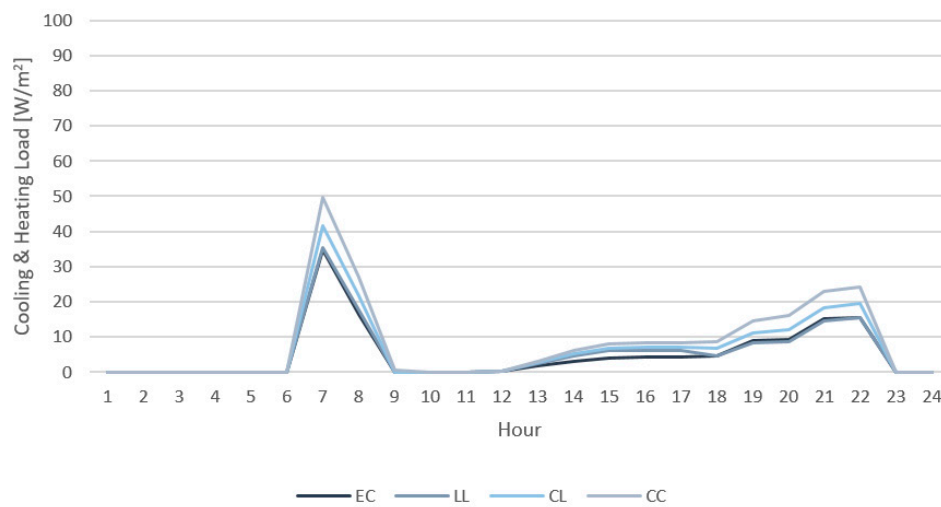
**Table 13.** Energy load of the east side on the spring equinox (cooling/heating) ( $W/m^2$ ).

Time	Electrochromic Smart Window (U-Value 1.1)						Architectural Window (U-Value 2.685, 1.771, 1.165)		
	EC (0.15)	EC (0.20)	EC (0.25)	EC (0.30)	EC (0.35)	EC (0.40)	CC (0.70)	CL (0.57)	LL (0.49)
1	0/0	0/0	0/0	0/0	0/0	0/0	0/0	0/0	0/0
2	0/0	0/0	0/0	0/0	0/0	0/0	0/0	0/0	0/0
3	0/0	0/0	0/0	0/0	0/0	0/0	0/0	0/0	0/0
4	0/0	0/0	0/0	0/0	0/0	0/0	0/0	0/0	0/0
5	0/0	0/0	0/0	0/0	0/0	0/0	0/0	0/0	0/0
6	0/0	0/0	0/0	0/0	0/0	0/0	0/0	0/0	0/0
7	0/37.058	0/35.85	0/35.556	0/34.933	0/35.18	0/34.858	0/49.546	0/41.63	0/35.307
8	0/18.004	0/16.896	0/16.577	0/16.436	0/16.913	0/17.002	0/26.954	0/21.633	0/17.525
9	0/0	0/0	0/0	0/0	0/0	0/0	0/0	0/0	0/0
10	0/0	0/0	0/0	0/0	0/0	0/0	0/0	0/0	0/0
11	0/0	0/0	0/0	0/0	0/0	0/0	0/0	0/0	0/0
12	0.107/0	0.116/0	0.126/0	0.135/0	0.145/0	0.147/0	0.209/0	0.178/0	0.16/0
13	1.531/1.277	1.666/0	1.802/0	1.939/0	2.08/0	2.104/0	3.005/0	2.56/0	2.296/0
14	3.11/0	3.388/0	3.668/0	3.952/0	4.242/0	4.293/0	6.154/0	5.234/0	4.689/0
15	3.998/0	4.354/0	4.714/0	5.077/0	5.449/0	5.515/0	7.896/0	6.72/0	6.021/0
16	4.143/0	4.511/0	4.883/0	5.259/0	5.643/0	5.71/0	8.172/0	6.956/0	6.234/0
17	4.148/0	4.517/0	4.889/0	5.265/0	5.649/0	5.717/0	8.181/0	6.963/0	6.241/0
18	2.95/2.111	3.211/1.516	3.474/1.534	3.74/1.35	4.013/1.101	4.06/0.841	5.804/2.711	4.943/1.701	4.431/0
19	0.55/9.658	0.598/8.842	0.647/8.935	0.696/8.756	0.747/8.555	0.756/8.091	1.078/13.331	0.919/10.22	0.824/7.353
20	0/10.287	0/9.61	0/9.791	0/9.772	0/9.724	0/9.284	0/16.109	0/12.143	0/8.613
21	0/15.665	0/15.096	0/15.311	0/15.403	0/15.433	0/15.038	0/22.903	0/18.395	0/14.549
22	0/16.02	0/15.491	0/15.735	0/15.915	0/16.032	0/15.66	0/24.303	0/19.418	0/15.359
23	0/0	0/0	0/0	0/0	0/0	0/0	0/0	0/0	0/0
24	0/0	0/0	0/0	0/0	0/0	0/0	0/0	0/0	0/0
Total	130.617	125.662	127.642	128.628	130.906	129.076	196.977	159.613	129.602

**Table 14.** Smart window g-value schedule for the east side on the spring equinox.

Time	1	2	3	4	5	6	7	8	9	10	11	12
g-value	0.15	0.15	0.15	0.15	0.15	0.15	0.40	0.30	0.40	0.40	0.40	0.15
Time	13	14	15	16	17	18	19	20	21	22	23	24
g-value	0.20	0.15	0.15	0.15	0.15	0.20	0.40	0.40	0.40	0.25	0.15	0.15

When the schedule was applied, the minimum value of the cooling and heating load was calculated as  $121.853 W/m^2$ , while those of the existing building windows CC, CL, and LL were  $196.977$ ,  $159.613$ , and  $129.602 W/m^2$ . Thus, the cooling and heating loads could be reduced by 6.0% to 38.1% when smart windows were used rather than control windows based on data from the eastern equinox. A graph comparing the energy load of the electrochromic window applied with the schedule to those of the control windows is shown in Figure 7.



**Figure 7.** Energy load comparison on the east side on the spring equinox.

### 3.2.2. Summer Solstice Analysis

On the summer solstice, only cooling energy was required. In all cases, it was confirmed that the lower the g-value, the lower the cooling load. The total daily cooling load is shown in Table 15.

**Table 15.** Energy load on the east side on the summer solstice (cooling) ( $W/m^2$ ).

Time	Electrochromic Smart Window (U-Value 1.1)						Architectural Window (U-Value 2.685, 1.771, 1.165)		
	EC (0.15)	EC (0.20)	EC (0.25)	EC (0.30)	EC (0.35)	EC (0.40)	CC (0.70)	CL (0.57)	LL (0.49)
1	6.013	6.551	7.098	7.654	8.225	8.327	12.019	10.195	9.111
2	5.94	6.469	7.007	7.553	8.114	8.214	11.858	10.05	8.984
3	5.705	6.204	6.711	7.226	7.755	7.849	11.278	9.578	8.574
4	5.365	5.789	6.221	6.666	7.127	7.207	10.245	8.732	7.843
5	5.302	5.72	6.14	6.567	7.004	7.077	9.998	8.529	7.669
6	5.336	5.757	6.18	6.61	7.051	7.127	10.129	8.637	7.754
7	5.536	6.004	6.482	6.973	7.478	7.567	10.837	9.216	8.258
8	5.827	6.342	6.866	7.398	7.944	8.041	11.562	9.82	8.79
9	9.501	10.869	11.473	12.726	13.587	14.001	20.041	16.855	15.32
10	6.889	7.593	8.003	8.71	9.243	9.358	12.967	11.113	9.962
11	6.696	7.451	7.937	8.705	9.298	8.794	12.974	10.512	9.36
12	6.387	7.002	7.377	7.998	8.516	8.37	11.837	9.897	9.021
13	5.763	6.279	6.586	7.099	7.503	7.708	10.547	9.117	8.336
14	5.983	6.493	6.796	7.307	7.698	7.87	10.703	9.297	8.481
15	6.058	6.569	6.867	7.369	7.751	7.918	10.735	9.304	8.515
16	6.217	6.735	7.035	7.543	7.928	8.09	10.924	9.492	8.688
17	6.598	7.122	7.417	7.929	8.312	8.488	11.313	9.891	9.091
18	6.217	6.717	7.003	7.49	7.856	8.051	10.69	9.382	8.638
19	5.698	6.097	6.481	6.886	7.287	7.37	9.946	8.676	7.923

Table 15. Cont.

Time	Electrochromic Smart Window (U-Value 1.1)						Architectural Window (U-Value 2.685, 1.771, 1.165)		
	EC (0.15)	EC (0.20)	EC (0.25)	EC (0.30)	EC (0.35)	EC (0.40)	CC (0.70)	CL (0.57)	LL (0.49)
20	5.445	5.841	6.202	6.601	6.984	7.079	9.549	8.336	7.616
21	5.227	5.613	5.964	6.352	6.726	6.818	9.215	8.039	7.341
22	6.287	7.116	7.189	8.008	8.303	9.1	11.094	10.181	9.943
23	6.474	7.07	7.678	8.295	8.928	9.038	12.986	11.03	9.874
24	6.401	6.987	7.585	8.192	8.816	8.928	12.836	10.907	9.767
Total	146.865	160.39	170.298	183.857	195.434	198.39	276.283	236.786	214.859

The daily cooling load of smart windows with a g-value of 0.15 was the lowest, at 146.865 W/m<sup>2</sup>. A schedule was also prepared, as shown in Table 16, because the g-value of 0.15 showed the best performance in all sections. The cooling loads for the control windows, CC, CL and LL, were 276.283, 236.786, and 214.859 W/m<sup>2</sup>. We found that application of the smart windows with the summer day schedule rather than control windows can reduce the cooling load by 31.6% to 46.8%. A graph comparing the energy load of the electrochromic window applied with the schedule to those of the control windows is shown in Figure 8.

Table 16. Smart window g-value schedule on the east side on the summer solstice.

Time	1	2	3	4	5	6	7	8	9	10	11	12
g-value	0.15	0.15	0.15	0.15	0.15	0.15	0.15	0.15	0.15	0.15	0.15	0.15
Time	13	14	15	16	17	18	19	20	21	22	23	24
g-value	0.15	0.15	0.15	0.15	0.15	0.15	0.15	0.15	0.15	0.15	0.15	0.15

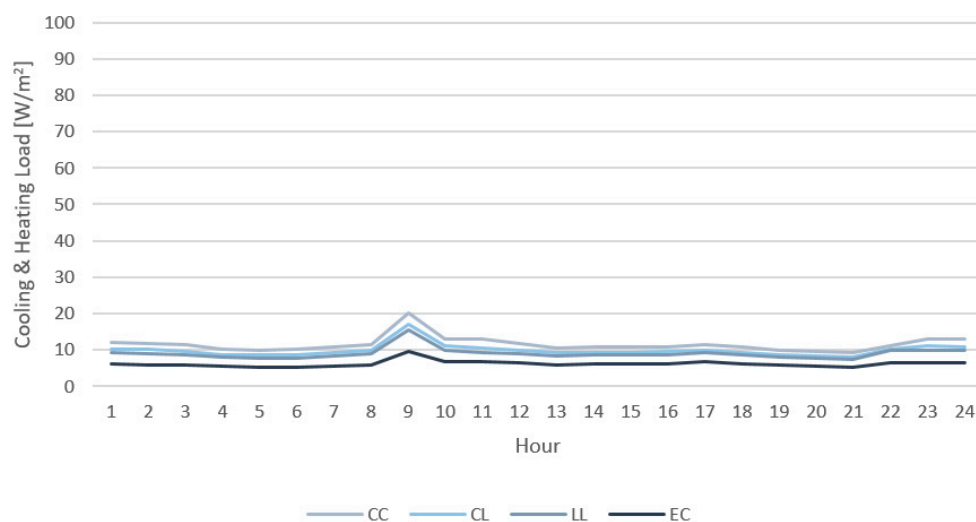


Figure 8. Energy load comparison on the east side on the summer solstice.

### 3.2.3. Autumnal Equinox Analysis

On the autumnal equinox, both cooling energy and heating energy were required, and the cooling load was higher than that on the spring equinox. The total daily cooling and heating load is shown in Table 17.



**Table 17.** Energy load on the east side on the autumnal equinox (cooling/heating) (W/m<sup>2</sup>).

Time	Electrochromic Smart Window (U-Value 1.1)						Architectural Window (U-Value 2.685, 1.771, 1.165)		
	EC (0.15)	EC (0.20)	EC (0.25)	EC (0.30)	EC (0.35)	EC (0.40)	CC (0.70)	CL (0.57)	LL (0.49)
1	2.354/0	2.564/0	2.776/0	2.991/0	3.21/0	3.248/0	4.653/0	3.959/0	3.547/0
2	2.468/0	2.687/0	2.908/0	3.131/0	3.36/0	3.4/0	4.864/0	4.141/0	3.711/0
3	1.794/0	1.952/0	2.111/0	2.273/0	2.438/0	2.467/0	3.524/0	3.002/0	2.692/0
4	1.332/0	1.453/0	1.574/0	1.698/0	1.824/0	1.846/0	2.654/0	2.255/0	2.018/0
5	1.329/0	1.45/0	1.572/0	1.696/0	1.822/0	1.845/0	2.655/0	2.254/0	2.017/0
6	0.8/0	0.871/0	0.943/0	1.016/0	1.091/0	1.104/0	1.581/0	1.345/0	1.205/0
7	0.642/9.473	0.689/9.096	0.738/8.616	0.788/8.333	0.84/8.086	0.847/7.391	1.224/14.805	1.031/10.171	0.925/6.801
8	1.722/0.266	1.876/0	2.031/0	2.189/0	2.349/0	2.378/0	3.408/0.203	2.899/0	2.597/0
9	3.959/0	4.277/0	4.604/0	4.936/0	5.507/0	5.568/0	7.661/0	6.639/0	6.062/0
10	4.76/0	5.098/0	5.434/0	5.779/0	6.131/0	6.187/0	8.42/0	7.317/0	6.66/0
11	4.76/0	5.098/0	5.434/0	5.779/0	6.131/0	6.187/0	8.42/0	7.317/0	6.66/0
12	4.76/0	5.098/0	5.434/0	5.779/0	6.131/0	6.187/0	8.42/0	7.317/0	6.66/0
13	4.76/0	5.098/0	5.434/0	5.779/0	6.131/0	6.187/0	8.42/0	7.317/0	6.66/0
14	4.76/0	5.101/0	5.445/0	5.8/0	6.165/0	6.224/0	8.59/0	7.415/0	6.722/0
15	4.76/0	5.103/0	5.46/0	5.83/0	6.209/0	6.272/0	8.688/0	7.494/0	6.785/0
16	4.766/0	5.121/0	5.484/0	5.857/0	6.239/0	6.302/0	8.732/0	7.531/0	6.818/0
17	4.76/0	5.103/0	5.449/0	5.807/0	6.175/0	6.235/0	8.614/0	7.432/0	6.735/0
18	4.76/0	5.098/0	5.434/0	5.779/0	6.131/0	6.187/0	8.42/0	7.317/0	6.66/0
19	4.76/0	5.1/0	5.44/0	5.788/0	6.144/0	6.201/0	8.459/0	7.344/0	6.68/0
20	4.676/0	5.034/0	5.39/0	5.744/0	6.105/0	6.164/0	8.42/0	7.317/0	6.65/0
21	3.76/0.234	4.093/0	4.43/0	4.771/0	5.119/0	5.181/0	7.413/0	6.31/0	5.655/0
22	2.974/0.679	3.237/0	3.504/0	3.773/0	4.049/0	4.098/0	5.863/0	4.991/0	4.473/0
23	2.575/0	2.803/0	3.033/0	3.266/0	3.504/0	3.546/0	5.071/0	4.317/0	3.87/0
24	2.228/0	2.425/0	2.624/0	2.825/0	3.03/0	3.066/0	4.383/0	3.732/0	3.346/0
Total	90.871	95.525	101.302	107.407	113.921	114.318	163.565	138.164	122.609

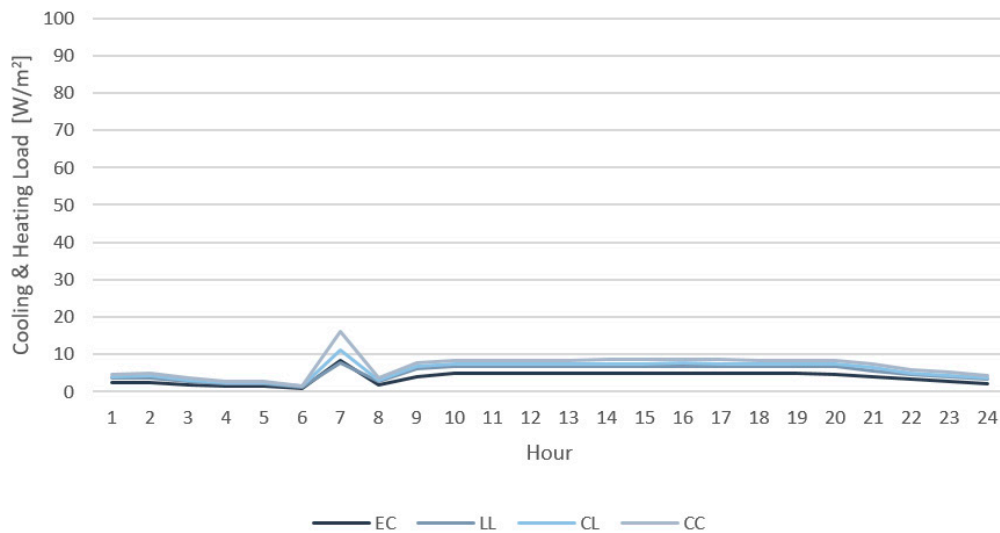
The g-value of smart windows that minimizes the load was derived for each hour, taking into account both cooling and heating energy. Excluding 6 to 8 o'clock and 21 to 22 o'clock, smart windows with a g-value of 0.15 were associated with the lowest cooling and heating loads. At 6 to 7 o'clock, a g-value of 0.40 was found to be the most advantageous, and at 7 to 8 o'clock, a g-value of 0.20 was found to be the most advantageous in terms of energy use. Also, a g-value of 0.20 was beneficial at 21–22 h. The final schedule is shown in Table 18.

**Table 18.** Smart window g-value schedule on the east side on the autumnal equinox.

Time	1	2	3	4	5	6	7	8	9	10	11	12
g-value	0.15	0.15	0.15	0.15	0.15	0.15	0.40	0.20	0.15	0.15	0.15	0.15
Time	13	14	15	16	17	18	19	20	21	22	23	24
g-value	0.15	0.15	0.15	0.15	0.15	0.15	0.15	0.15	0.15	0.20	0.15	0.15

When the schedule was applied, the minimum value of the cooling and heating load was calculated as 88.466 W/m<sup>2</sup>, while those of the existing building windows, CC, CL, and

LL, were 163.565, 138.164, and 122.609 W/m<sup>2</sup>. Thus, the cooling and heating loads could be reduced by 27.8–45.9% when smart windows were used rather than control windows based on data from the autumnal equinox on the east side of the building. A graph comparing the energy load of the electrochromic window applied with the schedule to those of the control windows is shown in Figure 9.



**Figure 9.** Energy load comparison on the east side on the autumnal equinox.

### 3.2.4. Winter Solstice Analysis

On the winter solstice, only heating energy was required. The total daily heating load is shown in Table 19.

**Table 19.** Energy load on the east side on the winter solstice (heating) (W/m<sup>2</sup>).

Time	Electrochromic Smart Window (U-Value 1.1)						Architectural Window (U-Value 2.685, 1.771, 1.165)		
	EC (0.15)	EC (0.20)	EC (0.25)	EC (0.30)	EC (0.35)	EC (0.40)	CC (0.70)	CL (0.57)	LL (0.49)
1	4.454	3.62	3.946	4.47	3.001	2.569	8.7	2.309	2.092
2	5.267	4.478	4.572	5.28	3.604	3.352	9.61	3.177	2.378
3	5.962	5.363	5.498	6.414	4.659	4.274	10.844	4.437	3.293
4	6.438	5.712	6.007	6.887	5.212	4.829	11.496	5.234	3.83
5	6.996	6.305	6.6	7.45	5.832	5.485	12.298	6.035	4.528
6	7.419	6.764	7.045	7.87	6.322	5.992	12.809	6.435	5.1
7	66.138	68.079	71.709	72.928	72.776	72.686	94.6	82.335	74.4
8	43.871	44.803	46.796	49.466	49.426	49.432	66.877	55.986	50.932
9	22.07	22.355	23.712	25.689	25.157	25.449	39.146	30.48	26.507
10	16.159	15.519	15.898	16.892	15.501	16.386	24.496	19.035	17.585
11	18.888	17.79	17.763	18.355	16.756	20.501	25.997	23.518	22.022
12	20.402	19.718	20.037	20.977	19.245	22.447	29.647	26.178	23.361
13	23.237	23.111	23.975	25.424	24.393	24.511	34.62	27.764	24.769
14	20.117	19.985	20.822	22.223	21.307	21.633	31.681	25.007	21.975
15	19.643	19.559	20.435	21.881	21.021	21.302	31.549	24.808	21.673
16	19.531	19.605	20.573	22.123	21.405	21.579	32.483	25.33	22.007

Table 19. Cont.

Time	Electrochromic Smart Window (U-Value 1.1)						Architectural Window (U-Value 2.685, 1.771, 1.165)		
	EC (0.15)	EC (0.20)	EC (0.25)	EC (0.30)	EC (0.35)	EC (0.40)	CC (0.70)	CL (0.57)	LL (0.49)
17	20.142	20.449	21.651	23.416	22.942	22.9	35.348	27.317	23.515
18	25.615	26.163	27.59	29.543	29.327	29.119	43.164	34.221	29.908
19	31.831	32.454	33.97	36.002	35.876	35.678	50.687	41.242	36.649
20	31.807	32.491	34.029	36.11	36.04	35.858	51.378	41.74	36.919
21	36.797	37.513	39.101	41.177	41.163	41.011	56.856	47.04	42.132
22	36.857	37.597	39.187	41.323	41.37	41.224	57.325	47.42	42.415
23	0.701	0	0	0	0	0	2.424	0	0
24	3.754	3.526	3.242	3.839	2.078	1.695	7.155	2.49	0.947
Total	494.096	492.959	514.158	545.739	524.413	529.912	781.19	609.538	538.937

When considering heating energy, the g-value of smart windows that can minimize the load for each hour was derived as shown in Table 20. From 0 to 6 o'clock, g-value of 0.40 was the best, and from 6 to 9 o'clock, g-value of 0.15 was the best. From 9 to 12 o'clock, g-value 0.35 had the least heating load, g-value 0.20 at 12 to 15 had the least heating load, and g-value 0.15 at 15 to 22:00 had the least heating load. Became. It was found that the heating load was 0 when the g-value was 0.20 or higher at 22–23 h, and the heating load was the lowest when the g-value was 0.40 at 23–24 h.

Table 20. Smart window g-value schedule on the east of the winter solstice.

Time	1	2	3	4	5	6	7	8	9	10	11	12
g-value	0.15	0.15	0.15	0.15	0.15	0.15	0.40	0.20	0.15	0.15	0.15	0.15
Time	13	14	15	16	17	18	19	20	21	22	23	24
g-value	0.15	0.15	0.15	0.15	0.15	0.15	0.15	0.15	0.15	0.20	0.15	0.15

When applying the schedule, the minimum value of the heating load was calculated as 477.012 W/m<sup>2</sup>. The existing architectural windows CC, CL, and LL were calculated as 781.19 W/m<sup>2</sup>, 609.538 W/m<sup>2</sup>, and 538.937 W/m<sup>2</sup>. It was found that the heating load can be reduced by 11.5% to 38.9% compared to general building windows based on the winter solstice period on the east side. The graph comparing the energy load of the electrochromic window applied with the schedule and the architectural window is as shown in the Figure 10.

### 3.3. West Side Analysis

#### 3.3.1. Spring Equinox Analysis

On the east side of the building on the spring equinox, both cooling energy and heating energy were required. The total daily cooling and heating load is shown in Table 21.

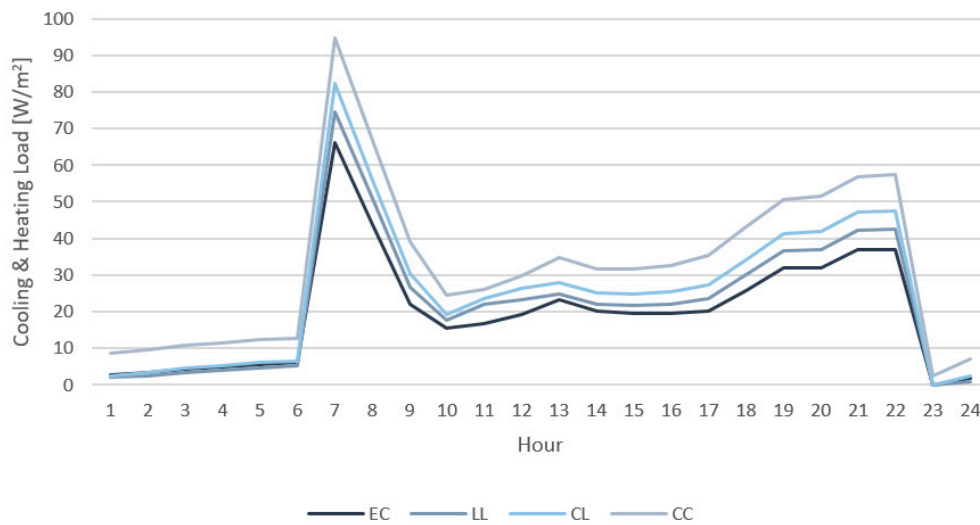


Figure 10. Energy load comparison on the east side on the winter solstice.

Table 21. Energy load on the west side on the spring equinox (cooling/heating) ( $W/m^2$ ).

Time	Electrochromic Smart Window (U-Value 1.1)						Architectural Window (U-Value 2.685, 1.771, 1.165)		
	EC (0.15)	EC (0.20)	EC (0.25)	EC (0.30)	EC (0.35)	EC (0.40)	CC (0.70)	CL (0.57)	LL (0.49)
1	0/0	0/0	0/0	0/0	0/0	0/0	0/0	0/0	0/0
2	0/0	0/0	0/0	0/0	0/0	0/0	0/0	0/0	0/0
3	0/0	0/0	0/0	0/0	0/0	0/0	0/0	0/0	0/0
4	0/0	0/0	0/0	0/0	0/0	0/0	0/0	0/0	0/0
5	0/0	0/0	0/0	0/0	0/0	0/0	0/0	0/0	0/0
6	0/0	0/0	0/0	0/0	0/0	0/0	0/0	0/0	0/0
7	0/36.692	0/36.116	0/35.682	0/35.017	0/34.851	0/34.682	0/48.189	0/40.664	0/34.403
8	0/22.499	0/22.255	0/22.133	0/21.963	0/22.418	0/22.488	0/34.898	0/28.266	0/23.624
9	0/5.135	0/4.867	0/4.746	0/4.585	0/5.006	0/5.142	0/16.932	0/10.671	0/6.293
10	0/4.045	0/3.774	0/3.64	0/3.492	0/3.863	0/4.044	0/15.197	0/9.334	0/5.235
11	0/2.902	0/2.57	0/2.389	0/2.297	0/2.519	0/2.835	0/12.955	0/7.825	0/4.1
12	0.11/1.565	0.12/1.201	0.13/0.963	0.139/0.882	0.149/1.246	0.152/1.701	0.218/9.63	0.186/5.533	0.167/2.509
13	1.576/2.664	1.717/2.316	1.859/2.265	2/2.249	2.144/2.45	2.177/2.654	3.14/9.139	2.667/5.826	2.401/3.23
14	3.201/0	3.492/0	3.784/0	4.077/0	4.373/0	4.44/0	6.43/1.783	5.454/1.825	4.903/0.241
15	4.116/0	4.488/0	4.863/0	5.238/0	5.617/0	5.703/0	8.251/0	7.001/0	6.296/0
16	4.265/0	4.65/0	5.037/0	5.425/0	5.817/0	5.906/0	8.618/0	7.247/0	6.518/0
17	4.271/0	4.656/0	5.043/0	5.431/0	5.824/0	5.912/0	8.754/0	7.255/0	6.525/0
18	3.037/0	3.31/0	3.584/0	3.858/0	4.136/0	4.199/0	6.062/0	5.149/0	4.633/0
19	0.566/6.306	0.617/5.872	0.668/5.452	0.718/3.884	0.77/2.569	0.782/1.834	1.127/0.883	0.957/0.874	0.862/0.594
20	0/8.646	0/8.547	0/8.265	0/7.177	0/6.053	0/5.331	0/5.911	0/4.801	0/3.412
21	0/14.407	0/14.314	0/14.358	0/13.576	0/12.797	0/12.204	0/15.246	0/12.938	0/10.789
22	0/14.992	0/14.891	0/15.117	0/14.592	0/14.027	0/13.534	0/18.209	0/15.1	0/12.5
23	0/0	0/0	0/0	0/0	0/0	0/0	0/0	0/0	0/0
24	0/0	0/0	0/0	0/0	0/0	0/0	0/0	0/0	0/0
Total	140.995	139.773	139.978	136.6	136.629	135.72	231.572	179.573	139.235

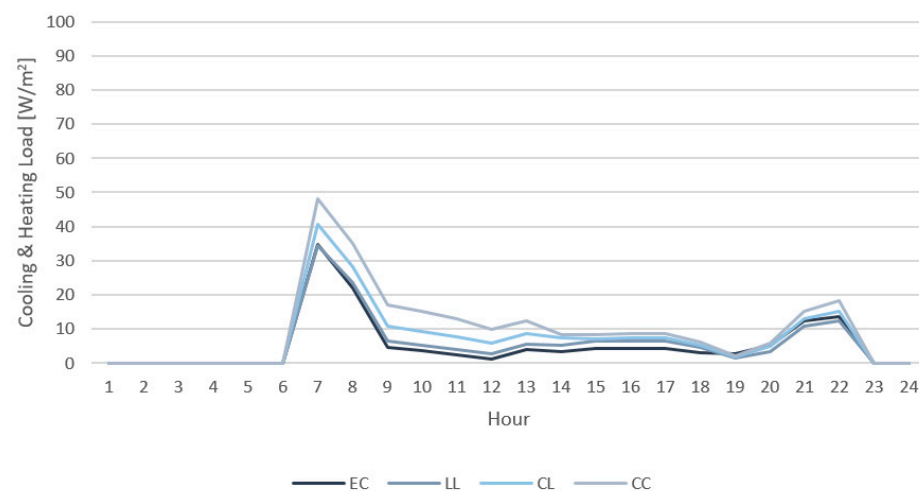
The g-value of smart windows that can minimize the load was derived for each hour, taking into account both cooling and heating energy. From 0 to 6 o'clock, the load was

calculated as 0 regardless of the g-value, and at 6 to 7 o'clock, a g-value of 0.40 was the best. From 7 to 12 o'clock, a g-value of 0.30 was the best. From 12 to 13 o'clock, a g-value of 0.20 was associated with the lowest load, and from 13 to 18 o'clock, a g-value of 0.15 was the most efficient. From 18 to 22 o'clock, a g-value of 0.40 corresponded to the lowest load, and after 22:00, the load was 0 regardless of the g-value. The final schedule is shown in Table 22.

**Table 22.** Smart window g-value schedule on the west side on the spring equinox.

Time	1	2	3	4	5	6	7	8	9	10	11	12
g-value	0.15	0.15	0.15	0.15	0.15	0.15	0.40	0.30	0.30	0.30	0.30	0.30
Time	13	14	15	16	17	18	19	20	21	22	23	24
g-value	0.20	0.15	0.15	0.15	0.15	0.15	0.40	0.40	0.40	0.40	0.15	0.15

When the schedule was applied, the minimum value of the cooling and heating load was calculated as  $124.648 \text{ W/m}^2$ . The values for the control windows, CC, CL, and LL, were 231.572, 179.573, and  $139.235 \text{ W/m}^2$ , respectively. Thus, the cooling/heating load could be reduced by 10.5% to 46.2% by the use of smart windows rather than control windows based on data from the spring equinox on the western side of the building. A graph showing the energy load of the electrochromic window applied with the schedule compared with those of the control windows is shown in Figure 11.



**Figure 11.** Energy load comparison on the west side on the spring equinox.

### 3.3.2. Summer Solstice Analysis

On the summer solstice, only cooling energy was required. In all cases, it was confirmed that the lower the g-value, the lower the cooling load. The total daily cooling load is shown in Table 23.

The daily cooling load of smart windows with a g-value of 0.15 was the lowest, at  $147.376 \text{ W/m}^2$ . In addition, the schedule was also prepared, as shown in Table 24. The g-value of 0.15 showed the best performance in all sections. The cooling loads for the control windows, CC, CL and LL, were 279.458, 239.468, and  $216.727 \text{ W/m}^2$ , respectively. Thus, use of the smart windows applied with the summer day schedule rather than control windows can reduce the cooling load by 32.0% to 47.3%. A graph comparing the energy load of the electrochromic window applied with the schedule to those of the control windows is shown in Figure 12.

**Table 23.** Energy load on the west side on the summer solstice (cooling) ( $W/m^2$ ).

Time	Electrochromic Smart Window (U-Value 1.1)						Architectural Window (U-Value 2.685, 1.771, 1.165)		
	EC (0.15)	EC (0.20)	EC (0.25)	EC (0.30)	EC (0.35)	EC (0.40)	CC (0.70)	CL (0.57)	LL (0.49)
1	6.19	6.752	7.321	7.894	8.478	8.612	12.561	10.624	9.529
2	6.116	6.668	7.228	7.791	8.365	8.496	12.394	10.474	9.396
3	5.877	6.396	6.923	7.455	7.995	8.118	11.787	9.979	8.966
4	5.535	5.977	6.424	6.881	7.349	7.454	10.704	9.097	8.198
5	5.471	5.906	6.343	6.781	7.224	7.321	10.444	8.885	8.015
6	5.505	5.944	6.384	6.825	7.272	7.372	10.582	8.997	8.107
7	5.706	6.193	6.689	7.194	7.71	7.826	11.324	9.602	8.635
8	6	6.538	7.083	7.631	8.189	8.316	12.109	10.24	9.193
9	6.701	7.306	8.155	8.548	8.679	8.808	11.456	10.417	9.7
10	5.798	6.114	6.489	6.884	7.267	7.355	9.86	8.643	7.96
11	6.107	6.437	6.768	7.128	7.52	7.607	10.132	8.905	8.215
12	6.162	6.507	6.856	7.198	7.549	7.617	10.169	8.918	8.214
13	5.669	6.02	6.372	6.725	7.126	7.212	9.797	8.536	7.826
14	5.935	6.37	6.81	7.264	7.749	7.401	10.238	8.611	7.929
15	6.549	7.156	7.772	8.392	9.022	8.273	12.331	9.91	8.788
16	7.394	8.05	8.721	9.396	10.105	9.952	14.532	12.136	10.729
17	7.602	8.263	8.934	9.611	10.313	10.341	14.941	12.603	11.367
18	6.591	7.115	7.645	8.176	8.723	8.864	12.419	10.685	9.736
19	5.996	6.515	7.04	7.565	8.105	8.242	11.682	10.012	9.086
20	5.617	6.019	6.427	6.84	7.26	7.377	10.183	8.822	8.06
21	5.375	5.767	6.159	6.552	6.95	7.464	9.68	8.955	8.157
22	6.233	7.057	7.654	8.343	9.265	9.402	13.151	11.564	10.387
23	6.661	7.284	7.916	8.553	9.201	9.346	13.57	11.491	10.323
24	6.586	7.199	7.82	8.447	9.086	9.233	13.412	11.362	10.211
Total	147.376	159.553	171.933	184.074	196.502	198.009	279.458	239.468	216.727

**Table 24.** Smart window g-value schedule on the west side on the summer solstice.

Time	1	2	3	4	5	6	7	8	9	10	11	12
g-value	0.15	0.15	0.15	0.15	0.15	0.15	0.15	0.15	0.15	0.15	0.15	0.15
Time	13	14	15	16	17	18	19	20	21	22	23	24
g-value	0.15	0.15	0.15	0.15	0.15	0.15	0.15	0.15	0.15	0.15	0.15	0.15

### 3.3.3. Autumnal Equinox Analysis

On the autumnal equinox, both cooling energy and heating energy were required, and the cooling load was greater than that on the spring equinox. The total daily cooling and heating load is shown in Table 25.

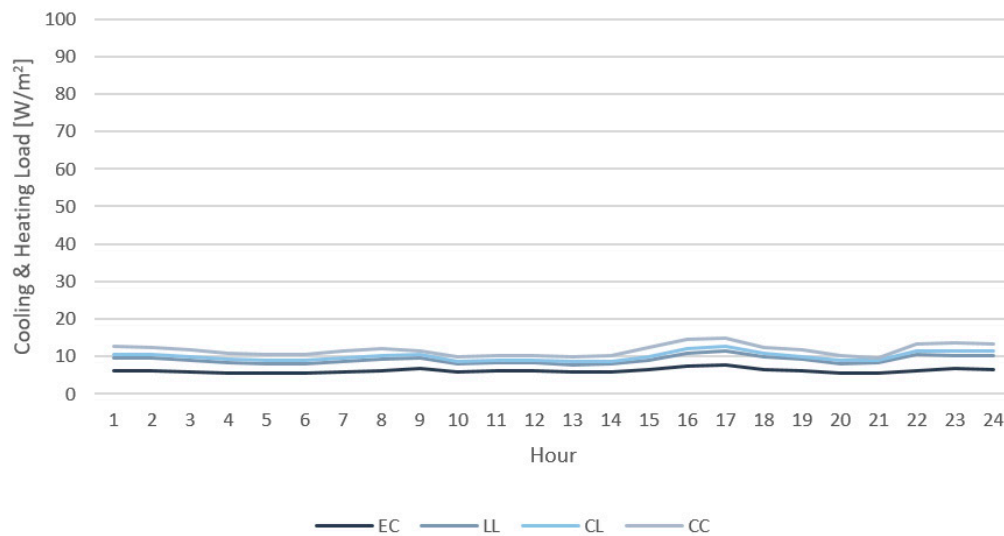


Figure 12. Energy load comparison on the west side on the summer solstice.

Table 25. Energy load on the west side on the autumnal equinox (cooling/heating) (W/m<sup>2</sup>).

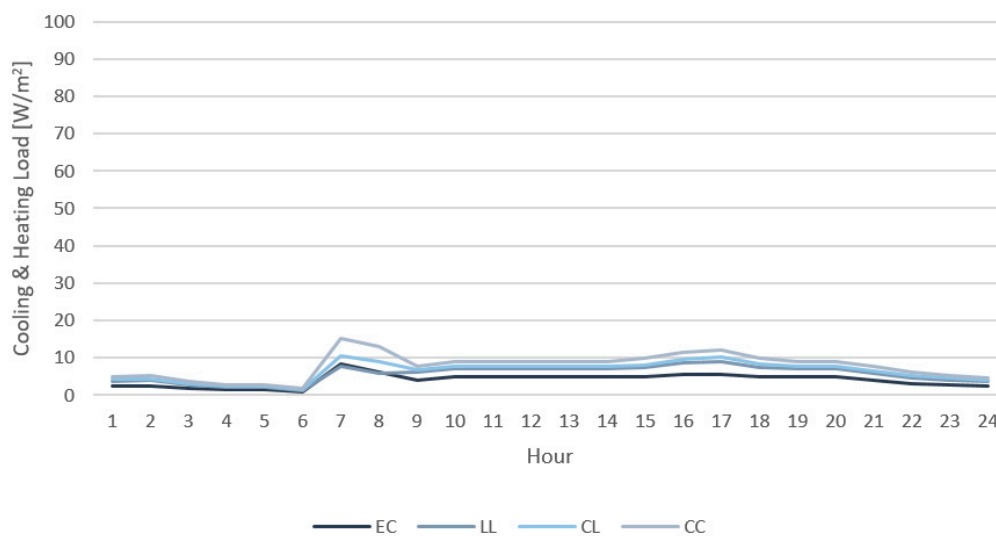
Time	Electrochromic Smart Window (U-Value 1.1)					Architectural Window (U-Value 2.685, 1.771, 1.165)			
	EC (0.15)	EC (0.20)	EC (0.25)	EC (0.30)	EC (0.35)	EC (0.40)	CC (0.70)	CL (0.57)	LL (0.49)
1	2.424	2.643	2.864	3.085	3.309	3.36	4.862	4.125	3.709
2	2.54	2.769	2.999	3.23	3.463	3.516	5.082	4.314	3.881
3	1.847	2.012	2.178	2.345	2.513	2.551	3.682	3.127	2.814
4	1.371	1.497	1.624	1.751	1.88	1.909	2.774	2.349	2.11
5	1.367	1.494	1.621	1.749	1.878	1.908	2.774	2.349	2.109
6	0.823	0.898	0.973	1.048	1.124	1.142	1.652	1.402	1.26
7	0.657/10.526	0.704/9.709	0.753/9.12	0.805/8.671	0.863/8.278	0.876/7.378	1.266/13.747	1.075/9.419	0.967/6.733
8	1.773/5.939	1.934/5.495	2.096/5.079	2.258/4.778	2.422/4.449	2.459/3.648	3.561/9.466	3.02/5.763	2.716/3.108
9	4.043	4.396	4.75	5.095	5.44	5.516	7.83	6.694	6.054
10	4.919	5.27	5.621	5.971	6.326	6.401	8.781	7.612	6.955
11	4.919	5.27	5.621	5.971	6.326	6.401	8.781	7.612	6.955
12	4.919	5.27	5.621	5.971	6.326	6.401	8.781	7.612	6.955
13	4.919	5.27	5.621	5.971	6.326	6.401	8.781	7.612	6.955
14	4.919	5.273	5.63	5.991	6.36	6.426	8.952	7.681	6.999
15	4.985	5.417	5.863	6.339	6.865	6.652	9.736	8.07	7.217
16	5.431	5.937	6.477	7.06	7.687	7.671	11.517	9.557	8.52
17	5.479	5.988	6.57	7.189	7.851	7.968	12.063	10.038	8.982
18	4.919	5.27	5.645	6.052	6.5	6.63	9.79	8.237	7.402
19	4.919	5.272	5.626	5.981	6.36	6.416	8.843	7.661	6.975
20	4.826	5.2	5.573	5.933	6.298	6.377	8.781	7.612	6.946
21	3.87	4.219	4.57	4.921	5.277	5.358	7.745	6.574	5.913
22	3.061	3.337	3.615	3.893	4.174	4.238	6.126	5.2	4.677
23	2.651	2.889	3.129	3.369	3.612	3.667	5.298	4.498	4.046
24	2.294	2.5	2.707	2.914	3.124	3.171	4.579	3.888	3.499
Total	100.34	105.933	111.946	118.341	125.031	124.441	185.25	153.101	134.457

The g-value of smart windows that can minimize the load was derived for each hour, taking into account both cooling and heating energy. Excluding 6 to 8 o'clock, smart windows with a g-value of 0.15 showed the lowest cooling and heating loads. From 6 to 8 o'clock, a g-value of 0.40 was the most advantageous. The final schedule is shown in Table 26.

**Table 26.** Smart window g-value schedule on the west side on the autumnal equinox.

Time	1	2	3	4	5	6	7	8	9	10	11	12
g-value	0.15	0.15	0.15	0.15	0.15	0.15	0.40	0.40	0.15	0.15	0.15	0.15
Time	13	14	15	16	17	18	19	20	21	22	23	24
g-value	0.15	0.15	0.15	0.15	0.15	0.15	0.15	0.15	0.15	0.15	0.15	0.15

When the schedule was applied, the minimum value of the cooling and heating load was calculated as 95.806 W/m<sup>2</sup>, while those of the existing building windows, CC, CL, and LL, were 185.25, 153.101, and 134.457 W/m<sup>2</sup>. Thus, the cooling and heating loads could be reduced by 28.7–48.3% by use of the smart windows rather than control windows based on data from the autumnal equinox on the west side of the building. A graph comparing the energy load of the electrochromic window applied with the schedule to that of the control windows is shown in Figure 13.



**Figure 13.** Energy load comparison on the west side on the autumnal equinox.

### 3.3.4. Winter Solstice Analysis

On the winter solstice, only heating energy was required. The total daily heating load is shown in Table 27.

The g-value of smart windows that can minimize the load was derived for each hour by considering the energy used for heat, as shown in Table 28. From 0 to 6 o'clock, a g-value of 0.40 was the best, and from 6 to 14 o'clock, a g-value of 0.15 was the best. At 14 to 17:00, a g-value 0.35 corresponded to the lowest heating load. At 17 to 22:00, a g-value of 0.20 was associated with the lowest heating load, and at 22 to 23:00, the load was 0 regardless of the g-value. From 23 to 24:00 h, the heating load was the lowest when the g-value was 0.40.



**Table 27.** Energy load on the west side on the winter solstice (heating) ( $W/m^2$ ).

Time	Electrochromic Smart Window (U-Value 1.1)						Architectural Window (U-Value 2.685, 1.771, 1.165)		
	EC (0.15)	EC (0.20)	EC (0.25)	EC (0.30)	EC (0.35)	EC (0.40)	CC (0.70)	CL (0.57)	LL (0.49)
1	4.232	4.38	3.325	3.681	2.544	1.52	5.842	3.779	0.793
2	5.082	4.921	4.236	4.141	3.298	2.529	6.976	4.868	1.022
3	5.804	5.937	5.005	5.338	4.327	3.541	8.398	6.128	2.28
4	6.284	6.43	5.549	5.889	4.912	4.02	9.279	6.916	2.669
5	6.856	7.005	6.154	6.496	5.588	4.722	10.171	7.736	3.445
6	7.291	7.437	6.652	6.985	6.102	5.272	10.715	8.111	4.079
7	66.575	71.038	72.136	72.638	73.156	72.792	93.176	83.759	74.946
8	44.77	46.749	47.639	49.796	50.676	50.186	66.646	59.321	51.839
9	26.844	28.731	29.547	31.609	32.363	32.042	48.025	40.984	33.674
10	25.166	26.88	27.556	29.467	30.116	29.921	44.963	38.463	31.515
11	23.69	25.151	25.627	27.31	27.735	27.753	41.335	35.617	29.178
12	22.773	24.1	24.479	26.014	26.328	26.405	39.103	33.836	27.736
13	24.544	25.863	26.211	27.724	27.891	27.67	40.147	34.809	28.972
14	20.327	20.676	20.19	20.872	20.138	24.353	31.463	31.577	26.36
15	15.81	15.34	14.103	13.947	12.733	17.758	21.334	22.71	20.346
16	12.671	12.386	11.298	11.295	10.298	11.341	17.093	15.005	12.124
17	14.948	15.049	14.376	14.744	14.134	14.123	21.264	18.103	14.183
18	24.47	25.388	25.428	26.536	26.562	26.001	36.586	31.778	26.377
19	31.551	32.75	33.101	34.489	34.786	34.228	46.912	41.046	34.988
20	31.76	33.053	33.525	34.993	35.428	34.912	48.494	42.224	35.878
21	36.897	38.274	38.809	40.374	40.869	40.371	54.493	47.969	41.457
22	37.063	38.468	39.067	40.675	41.243	40.775	55.309	48.575	41.972
23	0	0	0	0	0	0	1.434	0	0
24	4.095	3.968	2.569	2.54	1.5	0.957	4.354	3.148	0
Total	499.503	519.974	516.582	537.553	532.727	533.192	763.512	666.462	545.833

**Table 28.** Smart window g-value schedule on the west side on the winter solstice.

Time	1	2	3	4	5	6	7	8	9	10	11	12
g-value	0.40	0.40	0.40	0.40	0.40	0.40	0.15	0.15	0.15	0.15	0.15	0.15
Time	13	14	15	16	17	18	19	20	21	22	23	24
g-value	0.15	0.15	0.35	0.35	0.35	0.15	0.15	0.15	0.15	0.15	0.15	0.40

When applying the schedule, the minimum value of the heating load was calculated as  $475.956 W/m^2$ . The values for the control windows, CC, CL, and LL, were  $763.512$ ,  $666.462$ , and  $545.833 W/m^2$ . Thus, the heating load can be reduced by 12.8% to 37.6% by use of smart windows rather than control windows based on data from the winter solstice on the west side of the building. The graph comparing the energy load of the electrochromic window applied with the schedule to that of the control windows is shown in Figure 14.

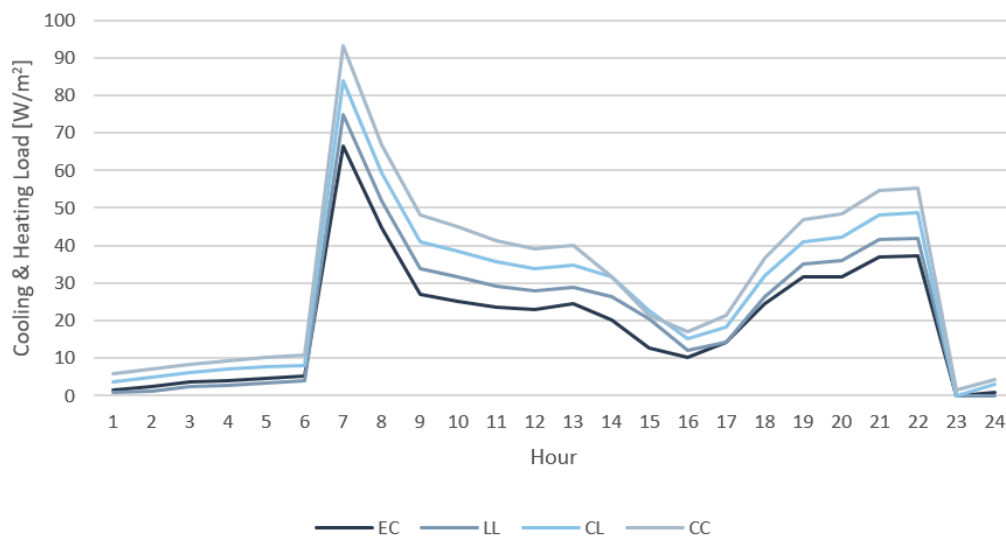


Figure 14. Energy load comparison on the west side on the winter solstice.

#### 4. Conclusions

The data on energy load per hour for electrochromic smart windows and existing windows under the as-developed schedules are shown in Table 29. Since the above schedules do not reflect special weather conditions, such as cloudy days, snow, and rain, the annual cooling and heating energy load was not calculated, and the load was summed for 4 sunny days representing each season.

Table 29. Total energy consumption ( $W/m^2$ ).

Direction	Window Type	Spring Equinox	Summer Solstice	Autumnal Equinox	Winter Solstice	Sum
South	EC	61.351	119.715	68.788	137.862	387.716
	CC	111.577	222.162	166.684	193.4	693.823
	CL	94.813	190.032	132.588	156.603	574.036
	LL	77.699	172.996	112.468	123.308	486.471
	Reduction rate	21.0–45.0%	30.8–46.1%	38.8–58.7%	–11.8–28.7%	20.3–45.0%
East	EC	121.853	146.865	88.466	477.012	834.196
	CC	196.977	276.283	163.565	781.19	1418.015
	CL	159.613	236.786	138.164	609.538	1144.101
	LL	129.602	214.859	122.609	538.937	1006.007
	Reduction rate	6.0–38.1%	31.6–46.8%	27.8–45.9%	11.5–38.9%	17.1–41.2%
West	EC	124.648	147.376	95.806	475.956	843.786
	CC	231.572	279.458	185.25	763.512	1459.792
	CL	179.573	239.468	153.101	666.462	1238.604
	LL	139.235	216.727	134.457	545.833	1036.252
	Reduction rate	10.5–46.2%	32.0–47.3%	28.7–48.3%	12.8–37.6%	18.6–42.2%

When comparing the derived cooling and heating loads, the cooling and heating loads of buildings with electrochromic smart windows were low for all seasons except winter. On the winter solstice, electrochromic smart windows were found to be more efficient than all control windows except the LL architectural windows on the south side.

On the spring equinox, the efficiency of smart windows on the eastern side of the building was somewhat insufficient compared to those on the south and west sides. The smart windows showed the maximum efficiency in comparison with the CC architectural windows on the west side, with a 46.2% reduction in the energy load for heating and cooling. For LL architectural windows on the eastern side, use of smart windows produced a 6% reduction in energy load for cooling and heating, the minimum reduction that was recorded.

On the summer solstice, a similar energy load reduction was found regardless of direction. Compared to CC architectural windows on the west side, the smart windows produced the maximum reduction in energy load for cooling and heating, at 47.3%. For LL architectural windows on the south side, smart windows showed a 30.8% reduction in cooling and heating energy loads, the minimum that was recorded.

On the autumnal equinox, smart windows on the south side were superior to those on the east and west sides. Compared to CC architectural windows on the south side, smart windows produced an energy savings for cooling and heating of 58.7%, the greatest savings among all control groups. Compared to LL architectural windows on the east side, smart windows produced an energy load reduction of 27.8%, representing the lowest energy load reduction rate in the autumn.

On the winter solstice, the reduction in energy load associated with use of smart windows on the east and west sides was superior to that on the south side. The smart windows were most efficient in comparison to the CC windows on the east side, at 38.9%. Compared to LL architectural windows on the south side, smart windows produced a rather low performance of  $-11.8\%$ .

The sum of the cooling and heating energy loads was derived for all four seasons. For the south side, energy savings of 20.3% to 45.0% are possible for each sunny day in all four seasons, making summer the season in which the greatest increase in energy efficiency is possible. Energy savings of 17.1–41.2% on the east side and 18.6–42.2% on the west side are possible. The energy load for each solar term is summarized in Figures 15–17.

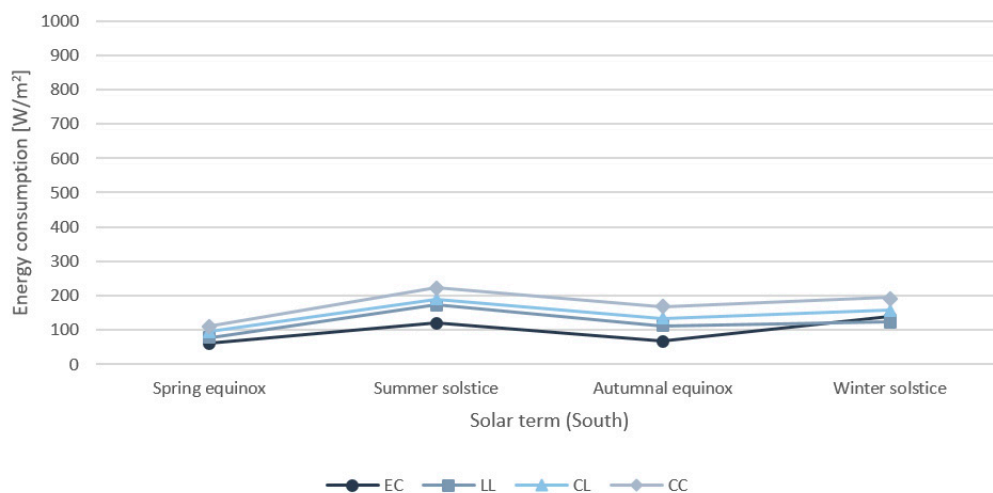
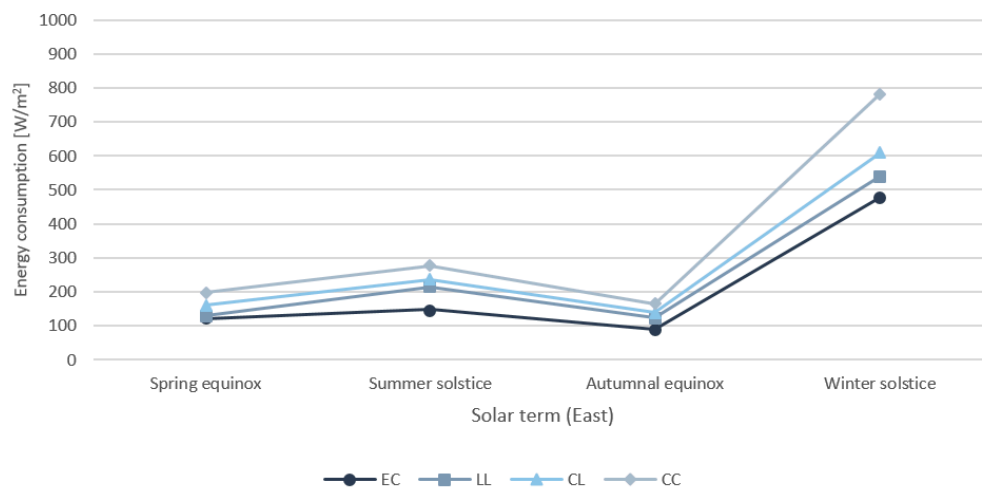
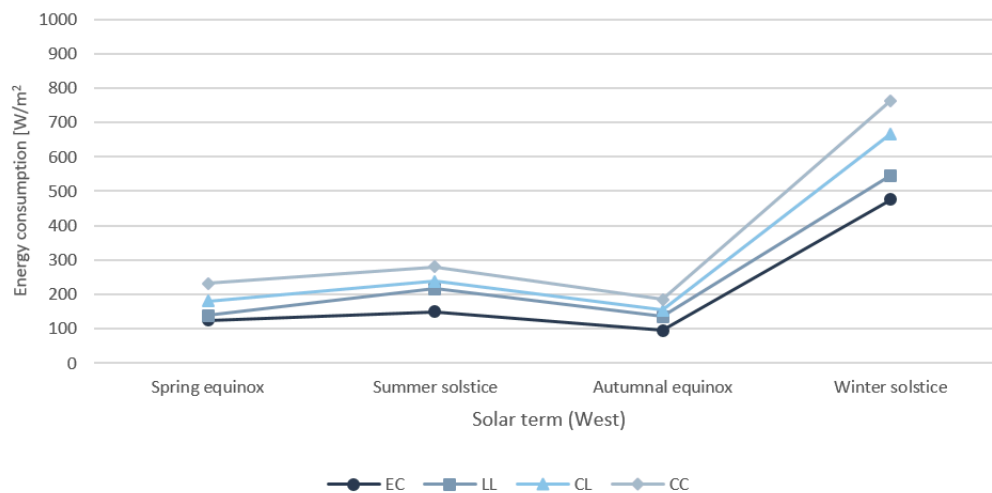


Figure 15. Energy consumption by solar term (south).



**Figure 16.** Energy consumption by solar term (east).



**Figure 17.** Energy consumption by solar term (west).

The significance of this study is as follows. First, it identifies the most efficient direction of a building to which electrochromic smart windows are applied. Second, the g-values of electrochromic smart windows can be changed, but there is no standard for which algorithm should be used to determine the g-value; thus, the schedule presented by this study is significant in that it can serve as a standard. In previous studies, energy efficiency or environmental analysis of smart windows was conducted through an analysis of annual data. For this reason, there was insufficient data on how electrochromic windows should be adjusted based on the time of day. Therefore, this study differs from previous studies in that it suggests the proper state of electrochromic windows according to time of day through the four seasons, which reflects the weather in the various seasons. Therefore, the study is significant in that it takes into account the controlled state of electrochromic windows in automated buildings. Third, it is meaningful in that it presents a method of calculating the energy performance required for the creation of the algorithm. In addition, the results of this study can be used as a standard for investigating the properties of smart windows.

This study has the following limitations. In smart windows, the g-value changes in conjunction with the VLT. A VLT that is too low does not sufficiently transmit sunlight through to the inside of the building, so the window does not serve as a window. Therefore, a minimum VLT standard that can provide indoor lighting is required. In addition, this study is limited in that the analysis was not conducted on all days of the year; energy analysis was performed only on the sunny days of the spring equinox, summer solstice,

autumn equinox, and winter solstice, representing the four seasons. Therefore, it is necessary to construct a database with more data measured on different days of the year. Alternatively, researchers could develop an algorithm to measure the energy consumption of buildings in real time and change the properties of smart windows. As a follow-up study, we will investigate methods of evaluating and controlling the lighting properties of smart windows.

**Author Contributions:** J.-H.K., J.H. and S.-H.H. designed the simulation settings; J.-H.K. and S.-H.H. performed the evaluations; J.-H.K. and S.-H.H. analyzed the data; J.H. and S.-H.H. verified the results; J.-H.K., J.H. and S.-H.H. wrote the paper. All authors have read and agreed to the published version of the manuscript.

**Funding:** This research was funded by National Research Foundation of Korea (Project No.: NRF-2018M3C1B9088457) and the Ministry of Trade, Industry and Energy of Korea (Project No.: 20193020010440).

**Institutional Review Board Statement:** Not applicable.

**Informed Consent Statement:** Not applicable.

**Data Availability Statement:** Data is contained within the article.

**Acknowledgments:** This paper has further been developed from Master's thesis by Jae-Hyang Kim. This research was supported by a grant from Future Leading Technology R&D Program managed by NRF, Korea and a grant from the R&D Program for Core Technology of Renewable Energy (Transparent Photovoltaic Cells Based on Nanophotonic Structures for Near-Infrared Control) through the Korea Institute of Energy Technology Evaluation and Planning (KETEP).

**Conflicts of Interest:** The authors declare no conflict of interest.

## References

1. Gran View Research. Smart Glass Market Size, Share & Trends Analysis Report by Technology (SPD, PDLC, Liquid Crystal, Electrochromic), by Application (Consumer Electronics, Architectural, Transportation), and Segment Forecasts. Available online: <https://www.grandviewresearch.com/industry-analysis/smart-glass-market> (accessed on 28 December 2020).
2. Martín-Chivelet, N.; Guillén, C.; Trigo, J.F.; Herrero, J.; Pérez, J.J.; Chenlo, F. Comparative Performance of Semi-Transparent PV Modules and Electrochromic Windows for Improving Energy Efficiency in Buildings. *Energies* **2018**, *11*, 1526. [CrossRef]
3. Abdelsalam, A. Conventional Fixed Shading Devices in Comparison to an Electrochromic Glazing System in Hot, Dry Climate. *Energy Build.* **2013**, *59*, 104–110.
4. Dussault, J.-M.; Gosselin, L. Office Buildings with Electrochromic windows: A Sensitivity Analysis of Design Parameters on Energy Performance, and Thermal and Visual Comfort. *Energy Build.* **2017**, *153*, 50–62. [CrossRef]
5. Kim, J.; Han, S. A Quantification Procedure for Interior Performance of Architectural Openings Associated with Dye-Sensitized Solar Cells. *Sustainability* **2019**, *11*, 6461. [CrossRef]
6. Nicholas, D.; Arman, S.; Stephen, S.; Delia, J. A Comparative Energy Analysis of Three Electrochromic Glazing Technologies in Residential Building. *Appl. Energy* **2017**, *192*, 95–109.
7. Oh, M.; Tae, S.; Hwang, S. Analysis of Heating and Cooling Loads of Electrochromic Glazing in High-Rise Residential Buildings in South Korea. *Sustainability* **2018**, *10*, 1121. [CrossRef]
8. Oh, M.; Jang, M.; Moon, J.; Roh, S. Evaluation of Building Energy and Daylight Performance of Electrochromic Glazing for Optimal Control in Three Different Climate Zones. *Sustainability* **2019**, *11*, 287. [CrossRef]
9. Detsi, M.; Manolitsis, A.; Atsonios, I.; Mandilaras, I.; Founti, M. Energy Savings in an Office Building with High WWR Using Glazing Systems Combining Thermochromic and Electrochromic Layers. *Energies* **2020**, *13*, 3020. [CrossRef]
10. Cannavale, A.; Ayr, U.; Fiorito, F.; Martellotta, F. Smart Electrochromic Windows to Enhance Building Energy Efficiency and Visual Comfort. *Energies* **2020**, *13*, 1449. [CrossRef]
11. Ghosh, A.; Norton, B.; Duffy, A. Behavior of an SPD switchable glazing in an outdoor test cell with heat removal under varying weather conditions. *Appl. Energy* **2016**, *180*, 695–706. [CrossRef]
12. Nundy, S.; Ghosh, A. Thermal and visual comfort analysis of adaptive vacuum integrated switchable suspended particle device window for temperate climate. *Renew. Energy* **2020**, *156*, 1361–1372. [CrossRef]
13. Min, J.; Hong, H. A Study on the Energy Performance Evaluation of a Smart Skin for Reducing Cooling Load of Building Envelope in Office Building. *Korean J. Air-Cond. Refrig. Eng.* **2018**, *30*, 546–557.
14. Ko, Y.; Hong, H.; Min, J. Energy Performance Evaluation of Responsive Smart Windows Applying SPD According to Window Area Ratio and SHGC Range. *Korean J. Air-Cond. Refrig. Eng.* **2020**, *32*, 441–447.
15. Ko, Y.; Oh, H.; Hong, H.; Min, J. Energy Consumption Verification of SPD Smart Window, Controllable According to Solar Radiation in South Korea. *Energies* **2020**, *13*, 5643. [CrossRef]

16. Baek, S.; Choi, W.; Suh, S. A Theoretical Study on a Folding Shading Device. *J. Korean Sol. Energy Soc.* **2009**, *29*, 28–36.
17. Park, J.; Kim, K. A Study on the Optimization of Glazing and Shading Devices for Energy Savings in Perimeter Zones of a Small Office Space. *J. Archit. Inst. Korea Plan. Des.* **2009**, *25*, 321–328.
18. Kim, T. LCC Evaluation of Multi-hybrid HVAC Systems in High-Rise Office Building Using Energy Analysis Method. Master's Thesis, University of Hanyang, Seoul, Korea, 2013.
19. Kim, G. A Basic Study on the Development of Air Cap Wall Module to Reduce Building Energy Consumption: Focusing on Amount Used Electric Power of Cooling, Heating, Lighting. Master's Thesis, University of Kookmin TED, Seoul, Korea, 2018.
20. ORION NES. Available online: <http://www.orionnes.co.kr/Vmodel> (accessed on 28 December 2020).
21. Yang, H. A Study on the Urban Fabric and the Typology of High-Rise Building on Teheran-Ro Street in Seoul. Master's Thesis, University of Seoul, Seoul, Korea, 2020.
22. Ministry of Land, Infrastructure, and Transport Notification No. 2017-881, Republic of Korea. Available online: [http://www.molit.go.kr/USR/I0204/m\\_45/dtl.jsp?idx=15270](http://www.molit.go.kr/USR/I0204/m_45/dtl.jsp?idx=15270) (accessed on 28 December 2020).